Westinghouse Non-Proprietary Class 3

WCAP-17609-NP
Revision 1

September 2012

Peach Bottom Units 2 and 3 Replacement Steam Dryer Structural Evaluation for High-Cycle Acoustic Loads

(Enclosure B.2)

Westinghouse

WCAP-17609-NP
Revision 1

Authors:

Leslie F. Wellstein*
Robert C. Theuret
David A. Suddaby
Charles Rajakumar
Garold W. Plonczak
Younus Munsi
Acoustics & Structural Analysis
Amir Salehzadeh
Piping Analysis and Fracture Mechanics

Editor:

Leslie F. Wellstein
Acoustics & Structural Analysis

Reviewer:

Yan Han*
Acoustics & Structural Analysis

September 2012

Approved by: **David R. Forsyth***, Manager
Acoustics & Structural Analysis

*Electronically approved records are authenticated in the electronic document management system.

Westinghouse Electric Company LLC
1000 Westinghouse Drive
Cranberry Township, PA 16066, USA

TABLE OF CONTENTS

LIST OF TABLES

LIST OF FIGURES

EXECUTIVE SUMMARY

High-cycle fatigue evaluations of the replacement steam dryer (RSD) for Peach Bottom Atomic Power Station (PBAPS) Units 2 and 3 have been completed using loads generated from Revision 4.1 of the Acoustic Circuit Model (ACM) methodology. Three acoustic resonance peaks have been observed in plant data obtained from the main steam lines (MSLs). These frequency peaks occur at [ ]^{a,c}. Acoustic loads and stresses for 102 percent of extended power uprate conditions have been evaluated for high-cycle fatigue.

The results of this evaluation indicate that the replacement steam dryer at EPU*1.02 plant conditions will meet the American Society of Mechanical Engineers (ASME) Boiler and Pressure Vessel (B&PV) Code Section III, Subsection NG high-cycle fatigue criteria. In addition, the results of this evaluation indicate that the replacement steam dryers at EPU*1.02 plant conditions will meet the present U.S. NRC guidelines. The smallest high-cycle fatigue stress ratio anywhere on the replacement steam dryer at Peach Bottom Unit 2 is [ ]^{a,c}. The smallest high-cycle fatigue stress ratio anywhere on the replacement steam dryer at Peach Bottom Unit 3 is [ ]^{a,c}. These results account for all the end-to-end biases and uncertainties in the loads, finite element model (FEM) and finite element analysis. Uncertainties in the modal frequency predictions of the finite element model are accounted for by including the stresses computed for loads that are shifted in the frequency domain by [ ]^{a,c}.

LIST OF ACRONYMS AND ABBREVIATIONS

3-D	three-dimensional
ACM	acoustic circuit model
APDL	ANSYS® Parametric Design Language
ASME	American Society of Mechanical Engineers
B&PV	boiler and pressure vessel
BWR	boiling water reactor
CLTP	current licensed thermal power
CSYS	coordinate system
DOF	degrees of freedom
EPU	extended power uprate
EPU*1.02	extended power uprate conditions multiplied by 1.02
FEM	finite element model
GA	gauge
IFT	inverse Fourier transform
MPC	multipoint constraints
MSL	main steam line
PBAPS	Peach Bottom Atomic Power Station
PSD	power spectral density
RSD	replacement steam dryer
SCF	stress concentration factor
SR	stress ratio
U.S. NRC	United States Nuclear Regulatory Commission

Trademark Note:

1 INTRODUCTION

In 2002, after increasing power to EPU conditions, a steam dryer in a boiling water reactor (BWR) experienced significant structural degradation. After extensive evaluation by various industry experts, the root cause of the dryer degradation was determined to be acoustic fluctuating pressure loads on the dryer, resulting from resonances produced by steam flow in the main steam lines (MSLs) across safety and relief valve inlets. The degradations found in the BWR steam dryer led to changes to Regulatory Guide 1.20 (Reference 3), requiring plants to evaluate their steam dryers before any planned increase in power level.

Exelon is planning an extended power uprate at PBAPS Units 2 and 3. An analysis has been performed to qualify the RSDs for acoustic pressure loads at EPU*1.02. The process used to perform the analysis involves multiple acoustic and structural analyses, scale model testing, and several computer codes, both commercially available and special-purpose codes developed in conjunction with the evaluation of acoustic loads.

This report documents the qualification of the PBAPS Units 2 and 3 RSDs subject to acoustic loads. The extent of this qualification of the dryer is to assess the potential for high-cycle fatigue. Structural qualification of the replacement steam dryer for the remaining duty cycle of events applicable to the PBAPS Units 2 and 3 operating system is documented in a separate report. Acoustic loads applicable to EPU*1.02 conditions are evaluated. A dynamic analysis was performed using a harmonic load methodology.

This WCAP provides results for EPU*1.02 conditions for loads developed using Revision 4.1 of the acoustic circuit model (ACM) (Reference 4).

The PBAPS Units 2 and 3 RSDs have similarity or are identical in many aspects. Unless specifically noted, the methods presented apply to both units.

Editorial changes have been incorporated into Revision 1. Revision bars have not been included.

2 METHODOLOGY

2.1 OVERVIEW

An analysis has been performed to assess the structural integrity of the replacement steam dryer for PBAPS Units 2 and 3 subject to acoustic loads. Acoustic loads applicable to EPU*1.02 conditions are evaluated. Analyses are performed to determine the acoustic loads on the replacement steam dryer. A dynamic analysis is performed using a harmonic load methodology that combines the use of a finite element representation of the dryer with special-purpose computer codes. The topics addressed in this report include the dryer finite element model (FEM), harmonic analysis, postprocessing, stress results, and design margins for the PBAPS Units 2 and 3 RSD.

2.2 DESIGN REQUIREMENTS

2.2.1 Endurance Strength Limit

The RSDs for PBAPS Units 2 and 3 are analyzed to the 2007 Edition of the ASME B&PV Code with the 2008 Addenda, Subsection NG[1] (Reference 1). Because the scope of this report is limited to the cyclic stresses developed as a result of acoustic loads, the governing criterion for the analysis is the allowable fatigue strength. The objective of this analysis is to show that the maximum alternating stress intensity anywhere in the dryer is less than the material endurance strength at 10^{11} cycles. The applicable fatigue curve for stainless steel (the RSD is manufactured from SS316L), is Figure I-9.2.2 in Appendix I of the Code.

[

]^{a,c}

The evaluation of the replacement steam dryer for non-acoustic loads is documented in a separate report.

2.2.2 Young's Modulus Correction

Before comparing the maximum alternating stress intensity to the ASME Code endurance strength, it is necessary to account for the Young's modulus correction. The analysis uses a Young's modulus of 25.45 x 10^6 psi, compared to the value to construct the fatigue curves of 28.3 x 10^6 psi. The ratio that is applied to the calculated alternating stress intensities is 1.112 (28.3/25.45).

1. Hereafter referred to as the Code or the ASME Code.

2.3 DRYER GEOMETRY

Plots of the replacement steam dryers are shown in Figures 2-1 through 2-3.

a,c

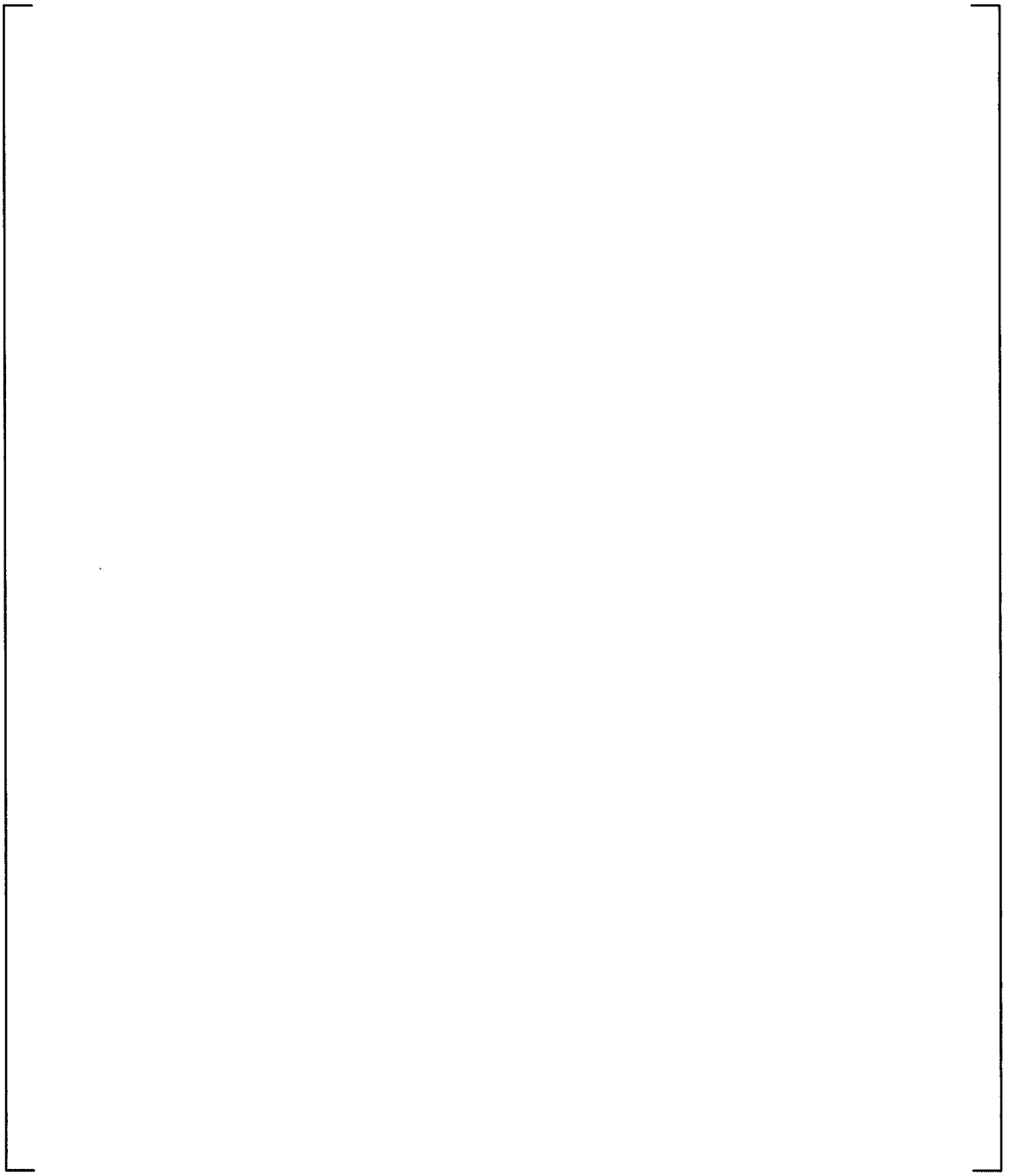

Figure 2-1 Peach Bottom Unit 2 Replacement Steam Dryer

a,c

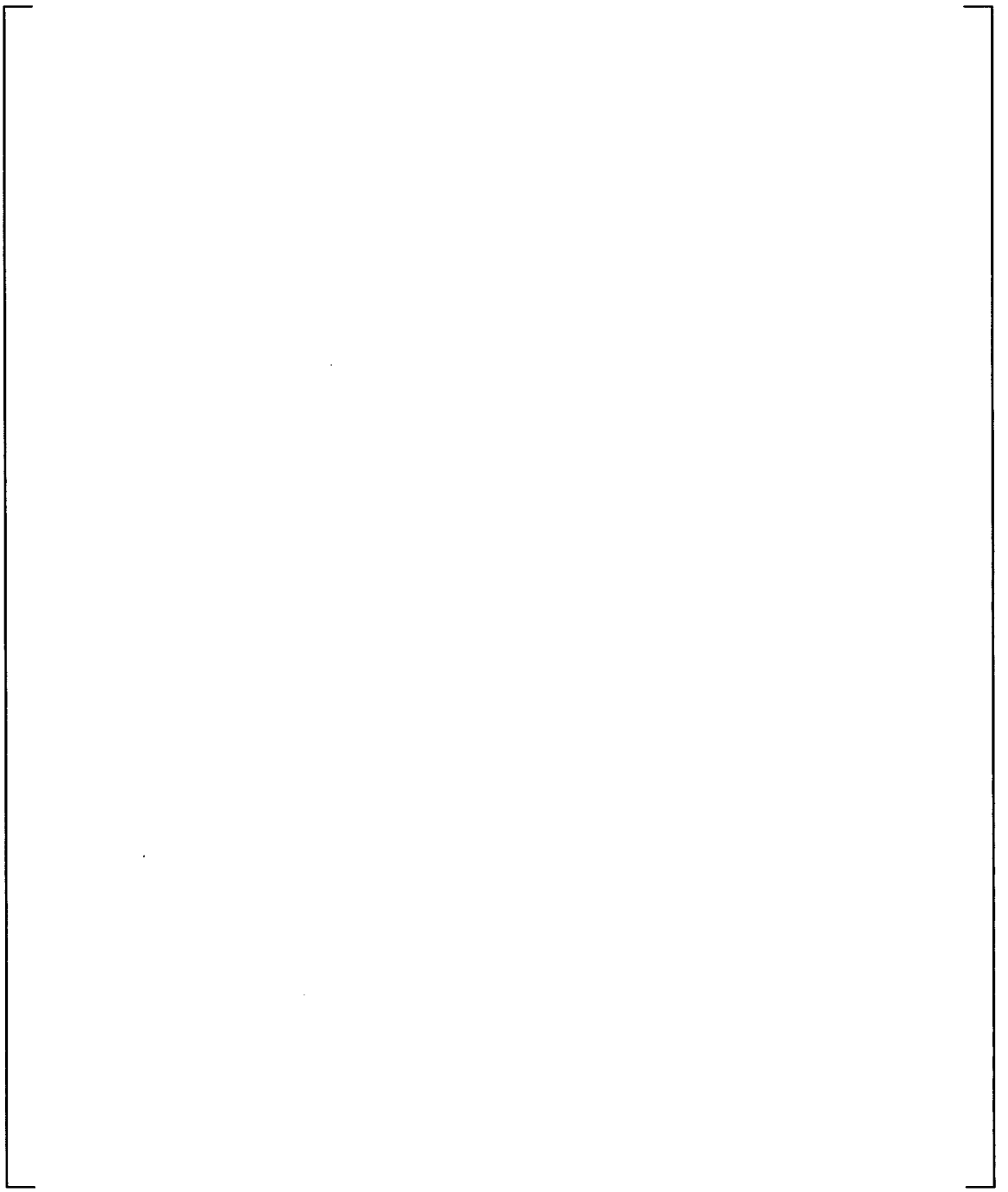

Figure 2-2 Peach Bottom Unit 2 Replacement Steam Dryer with Instrumentation Mast

a,c

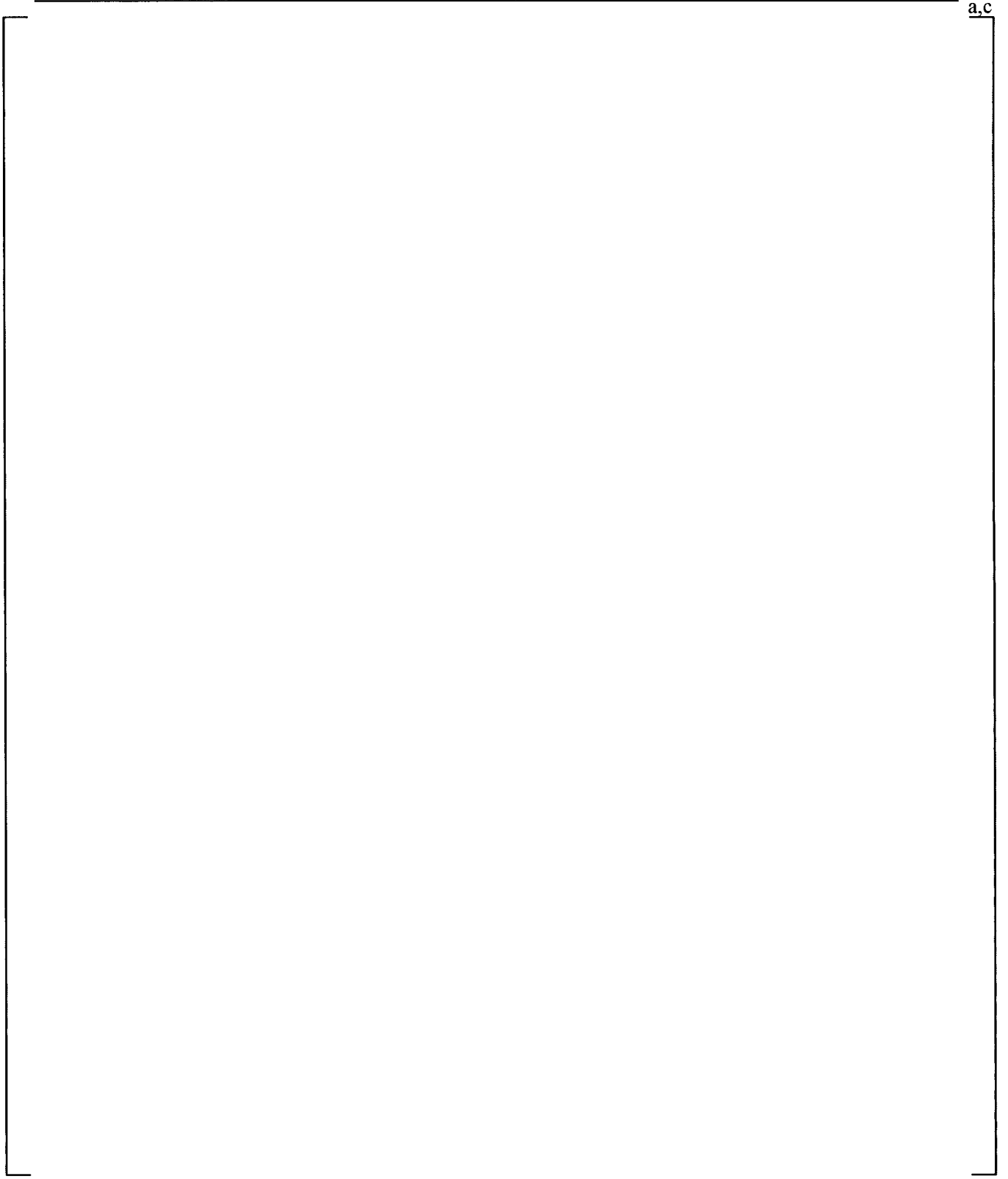

Figure 2-3 Peach Bottom Unit 3 Replacement Steam Dryer

3 FINITE ELEMENT MODEL

3.1 MODEL DESCRIPTION

The Peach Bottom Units 2 and 3 replacement steam dryer FEMs were built with *ANSYS*® using the ANSYS Parametric Design Language (APDL). There are three finite element models used in this evaluation: Peach Bottom Unit 2 without the instrumentation mast, Peach Bottom Unit 2 with the instrumentation mast, and Peach Bottom Unit 3. The differences between the units are:

- Peach Bottom Unit 2 has the instrumentation mast and the associated brackets on the dryer top girders for attaching the mast. Peach Bottom Unit 3 does not have an instrumentation mast. Note that in the future, the instrumentation mast at Peach Bottom Unit 2 will be removed.

- Peach Bottom Unit 2 has two sets of rods, lifting and hold-down rods, and therefore a different design of the lifting bracket that attaches the rods to the top plate of the outer ring vane bank.

The finite element models consist mostly of [

]^{a,c}

Additionally, [

]^{a,c}. The ANSYS SHELL63 structural elements are not capable of accepting as input complex (real and imaginary) loads. In this case, [

]^{a,c}.

The octagonal dryer structure includes [

]^{a,c}

The support ring has [

]^{a,c}

The [

]^{a,c}

Figure 3-11 shows the lifting rod arrangement for Peach Bottom Unit 2. Unit 3 has a similar arrangement but without the hold-down rods (Figure 3-14).

Figure 3-12 shows details of the [

].^{a,c}

Peach Bottom Unit 2 FEM with the instrumentation mast has [

]^{a,c}

3.1.1 Element Types

The dryer finite element model is composed of [

]^{a,c}

3.1.2 Element Connectivity

The dryer plates are [

]^{a,c}

[

]^{a,c}

[

]^{a,c} The vane bank is discussed in more detail in subsection 3.1.3. The lifting and hold-down rods are attached to brackets that weld to the vane bank top plate (Figures 3-10, 3-11 and 3-16).

3.1.3 Vane Bank Representation

The vane bank modules are box-like structures with many internal hanging chevrons. [

]^{a,c}

3.1.4 Dryer Skirt Submerged in Water

The dryer skirt is partially submerged in water. In the FEM, the skirt is separated into components above and below the water line. The acoustic loading is only applied to elements above the water line. The material density for the stainless steel below water has been adjusted to account for the effect of the hydrodynamic mass. [

]^{a,c}

3.2 MODEL BOUNDARY CONDITIONS

During dryer installation, the structure is leveled relative to the lugs so that all lugs are equally contacted by the dryer. The support lug centerlines are located at the following angular measurements on the support ring: azimuths 4 degrees, 94 degrees, 184 degrees, and 274 degrees. The model is restrained [

]^{a,c}

a,c

Figure 3-1 Peach Bottom Steam Dryer FEMs: [ ][a,c]

a,c

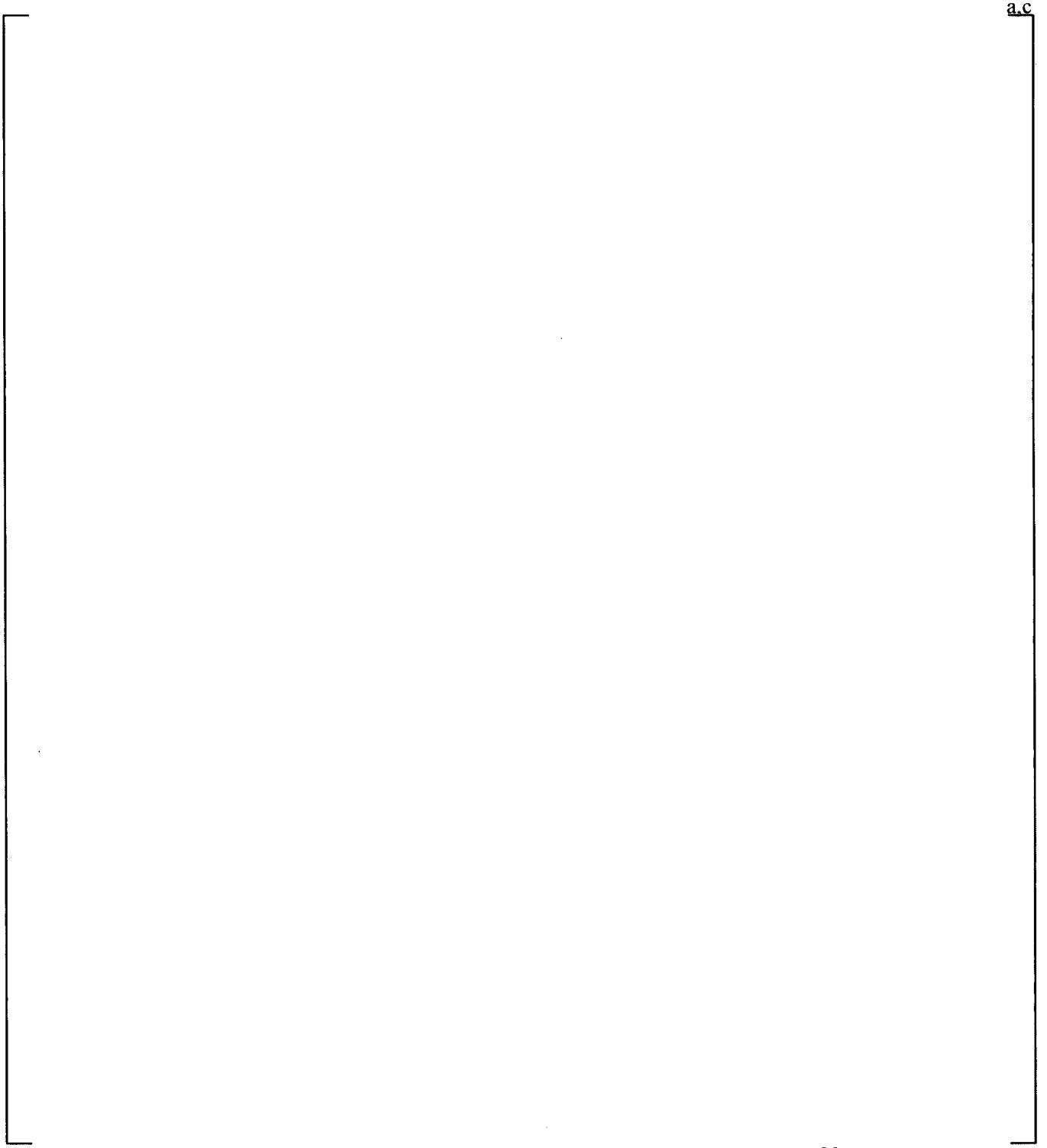

Figure 3-2 Peach Bottom Steam Dryer FEMs: [ ]^{a,c}

a,c

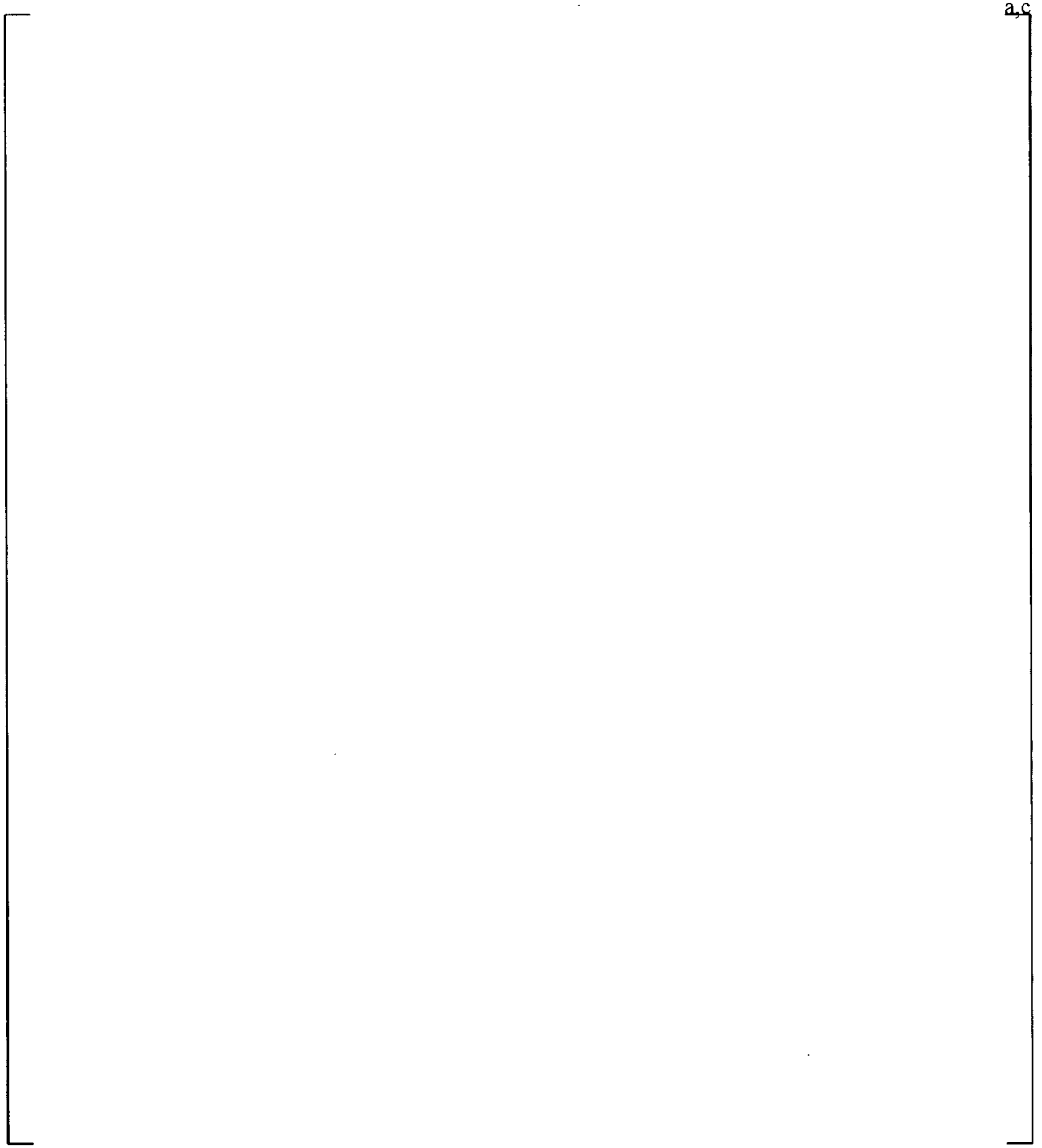

Figure 3-3 Peach Bottom Steam Dryer FEMs: [ ]^{a,c}

a,c

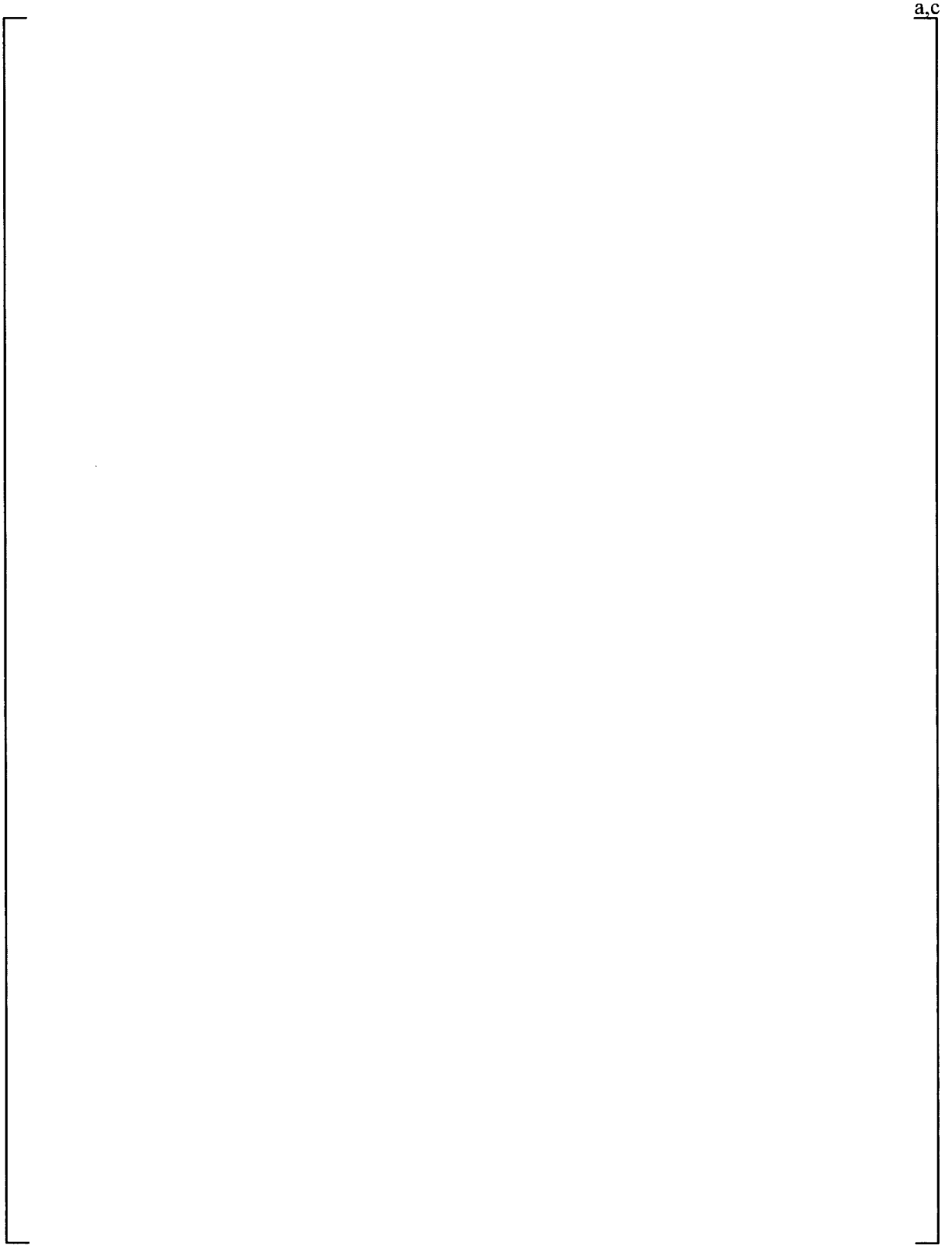

Figure 3-4 Peach Bottom Steam Dryer FEMs: [ ]^{a,c}

a,c

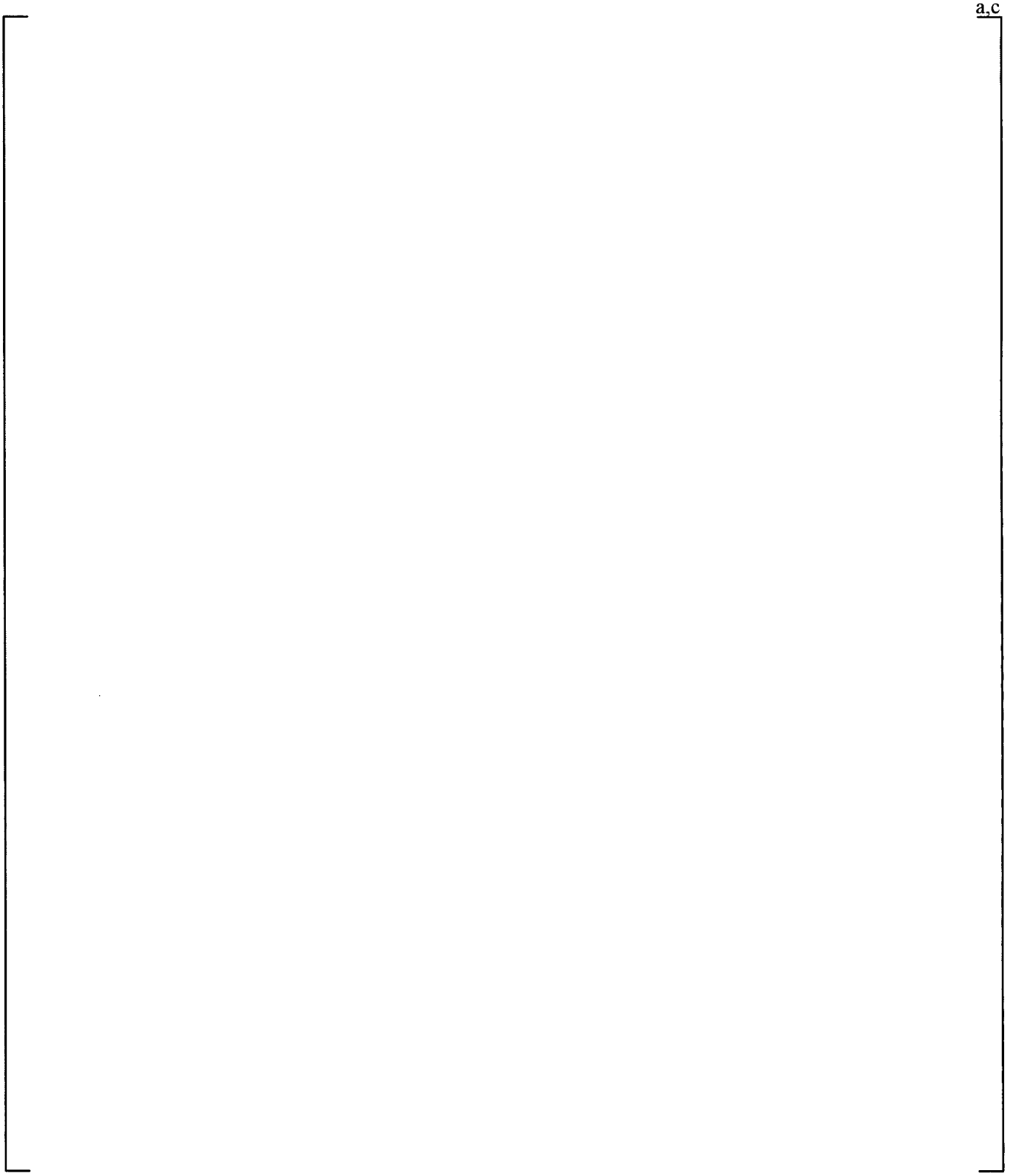

Figure 3-5 Peach Bottom Steam Dryer FEMs: [ ]^{a,c}

a,c

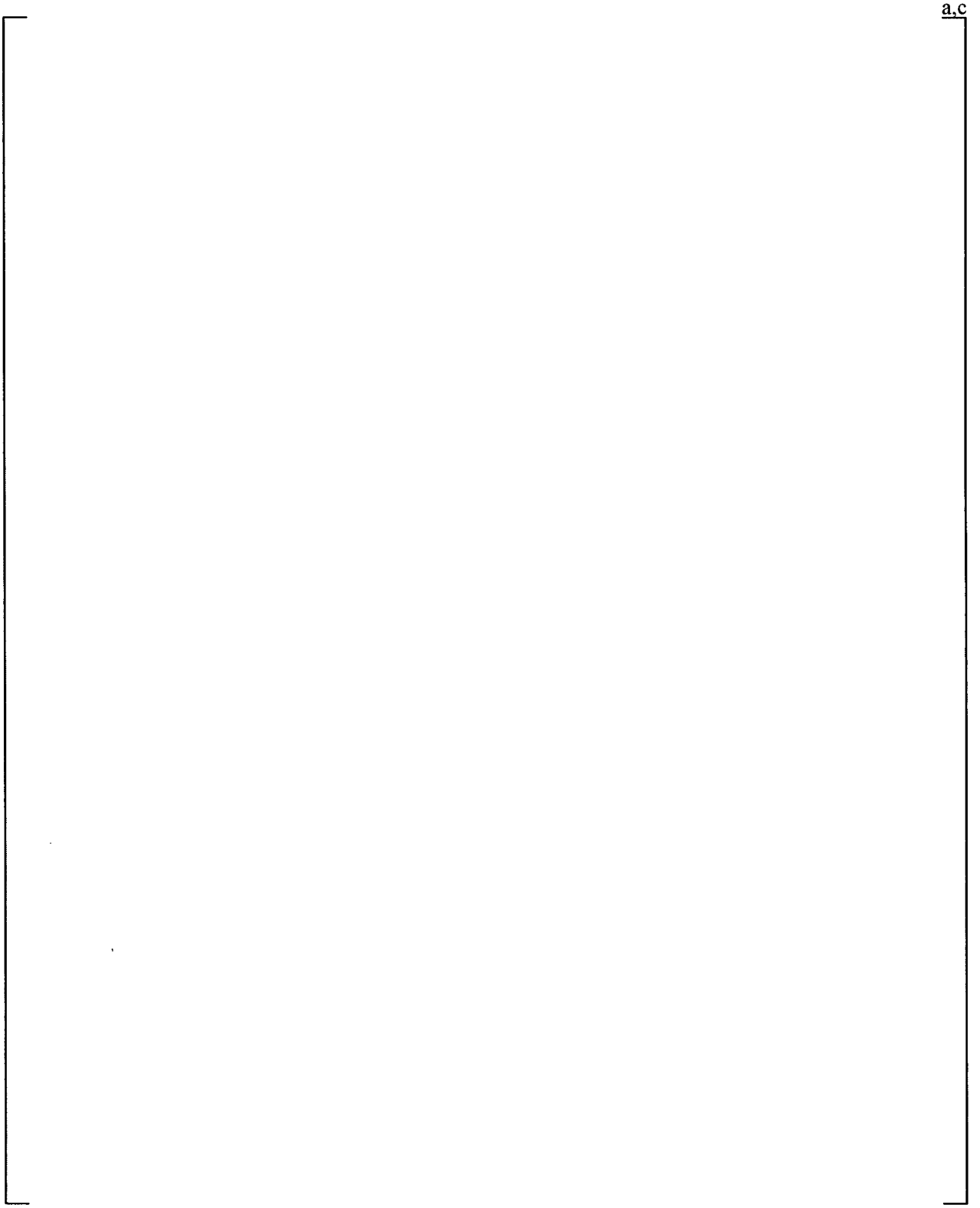

Figure 3-6 Peach Bottom Steam Dryer FEMs: [ ]^{a,c}

a,c

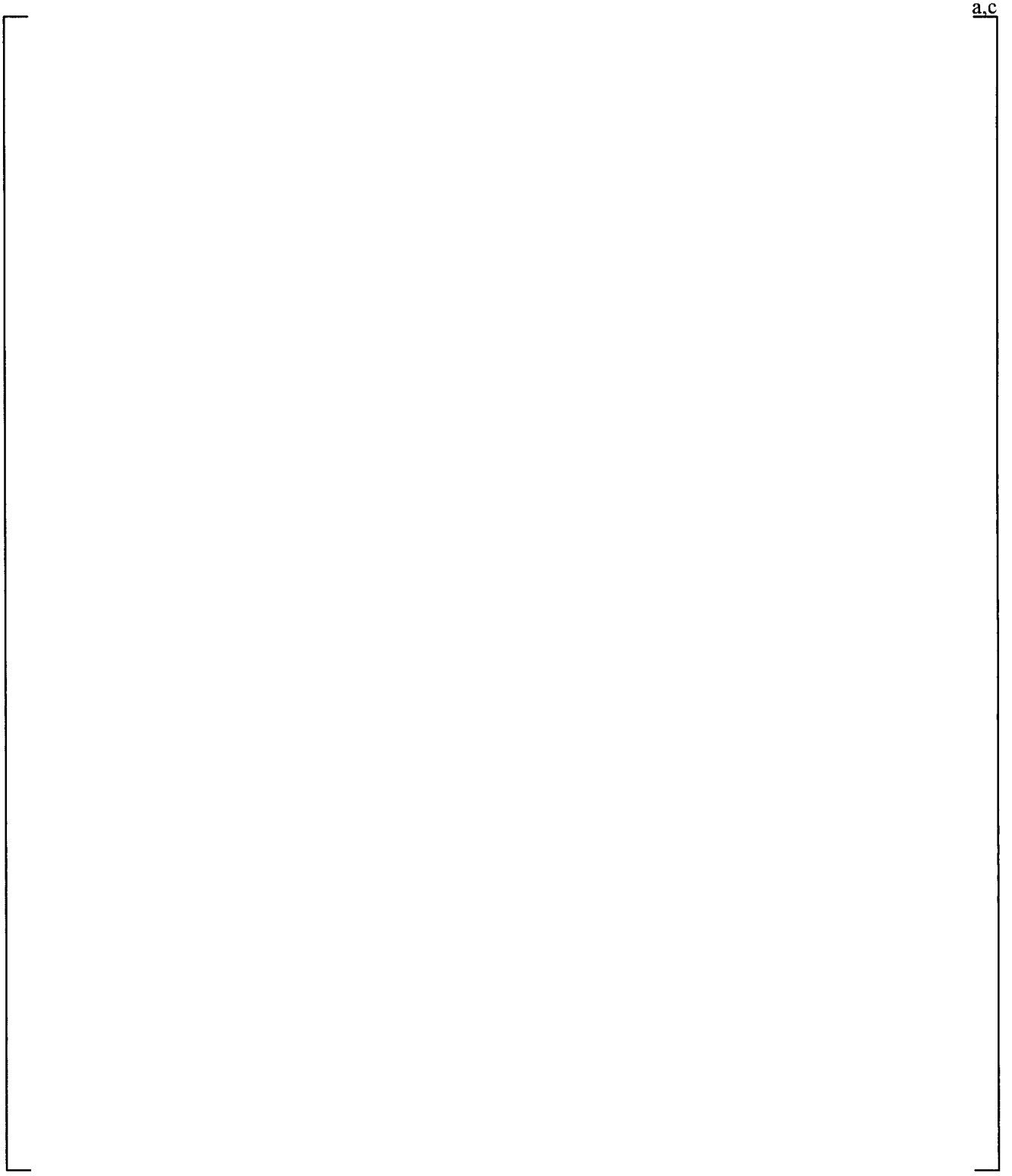

Figure 3-7 Peach Bottom Steam Dryer FEMs: [ ]^{a,c}

a,c

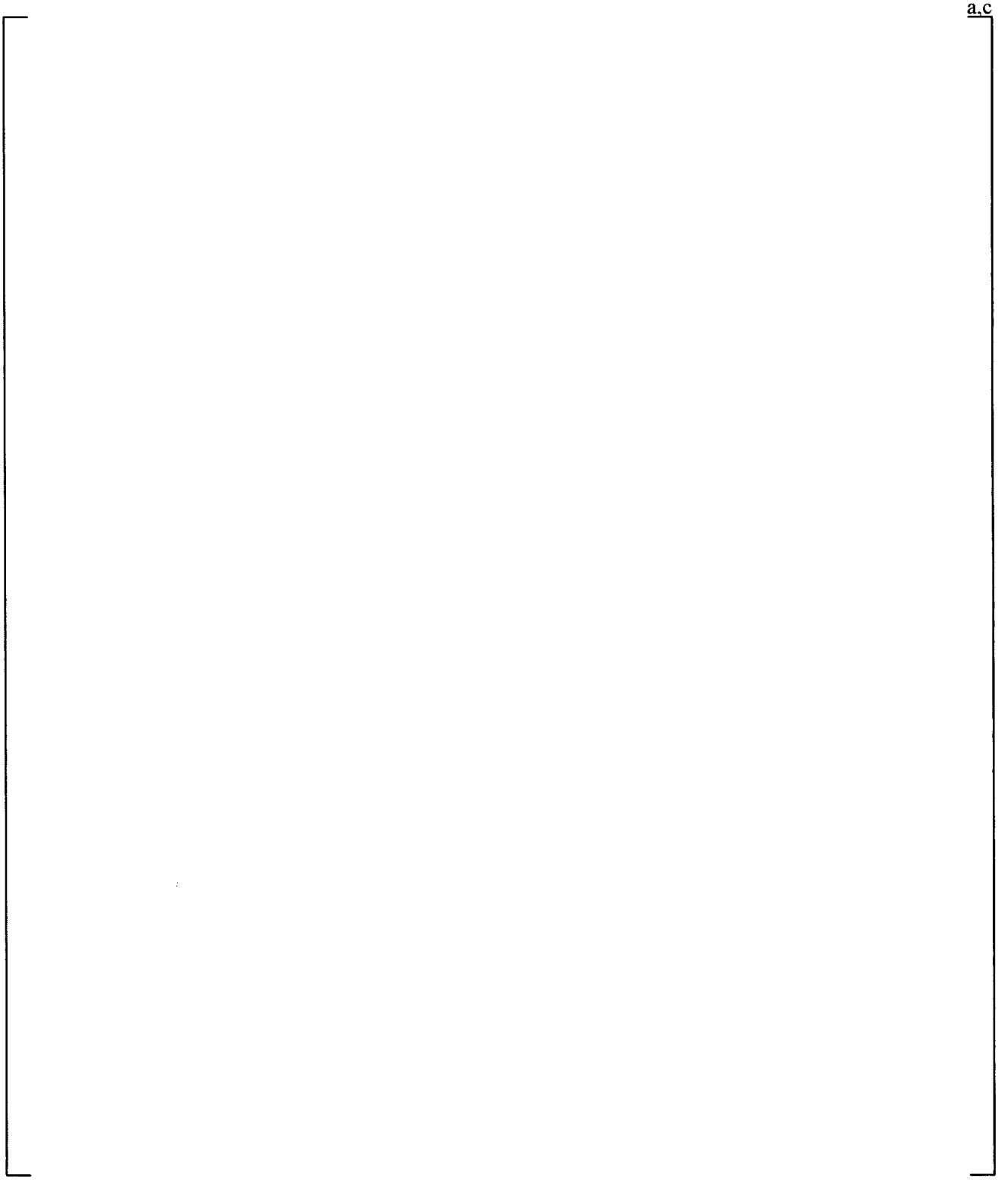

Figure 3-8 Peach Bottom Steam Dryer FEMs: [ ]a,c

a,c

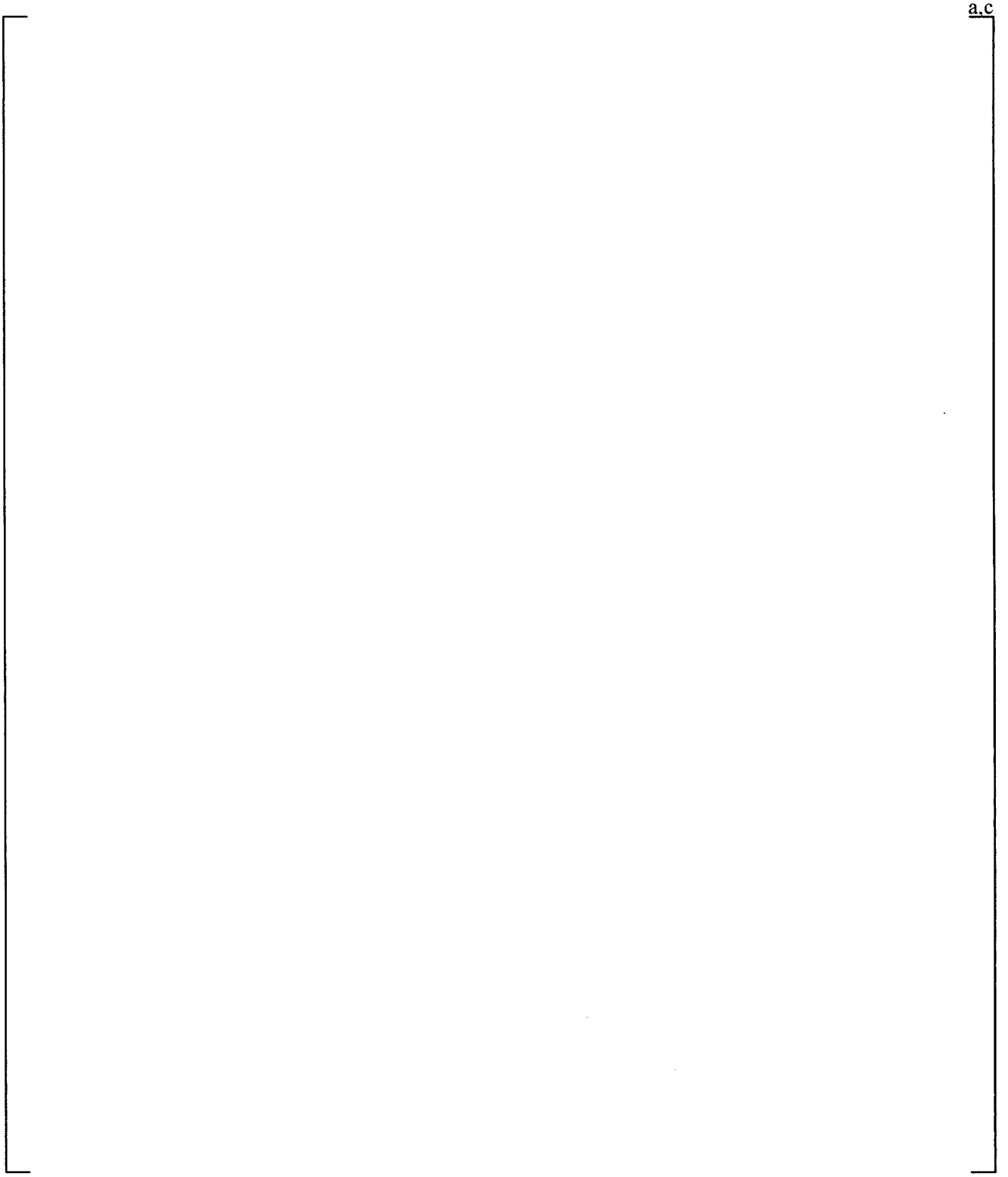

Figure 3-9 Peach Bottom Steam Dryer FEMs: [ ]^{a,c}

a,c

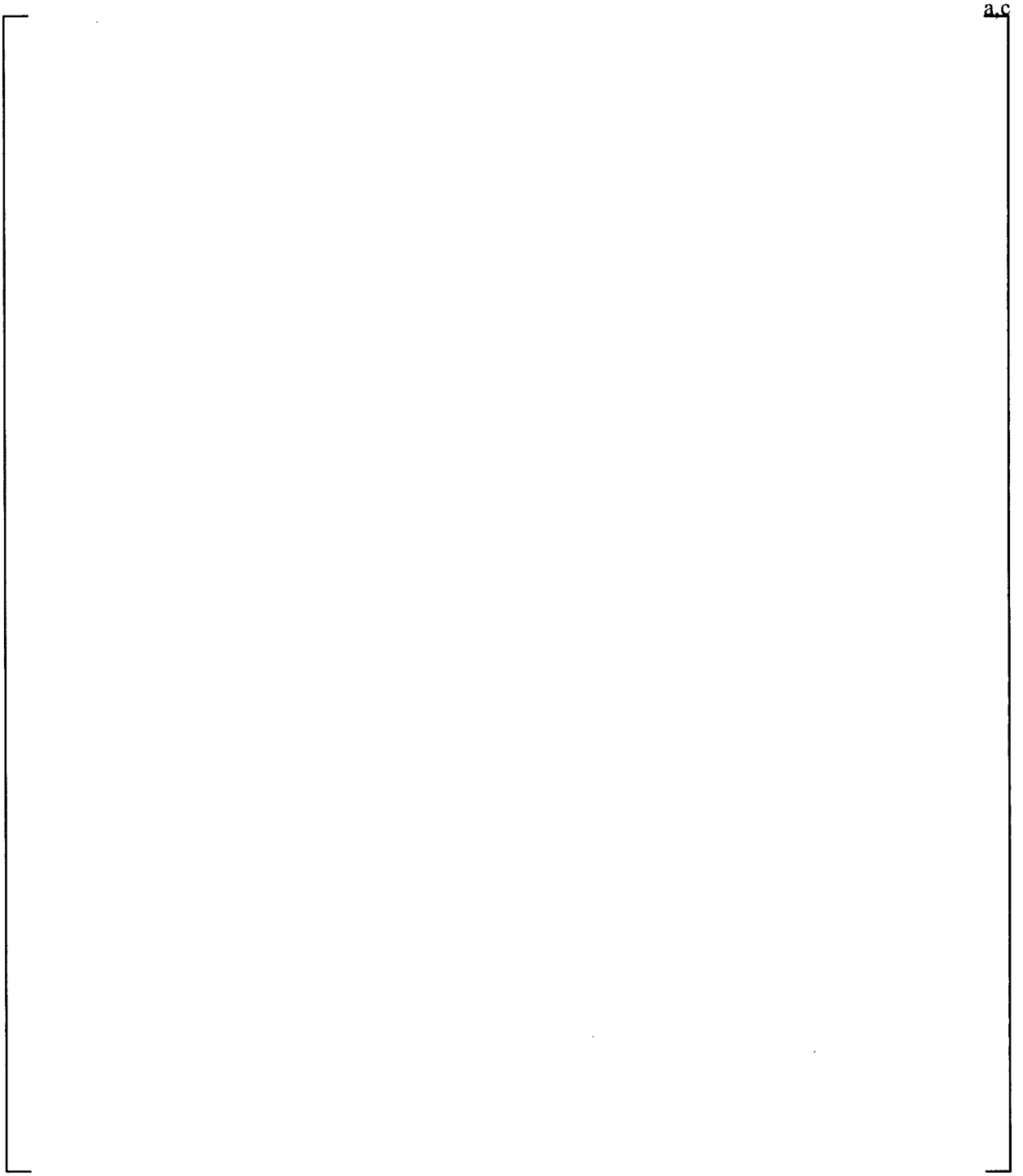

Figure 3-10 Peach Bottom Unit 2 Steam Dryer FEM: View from Below

a,c

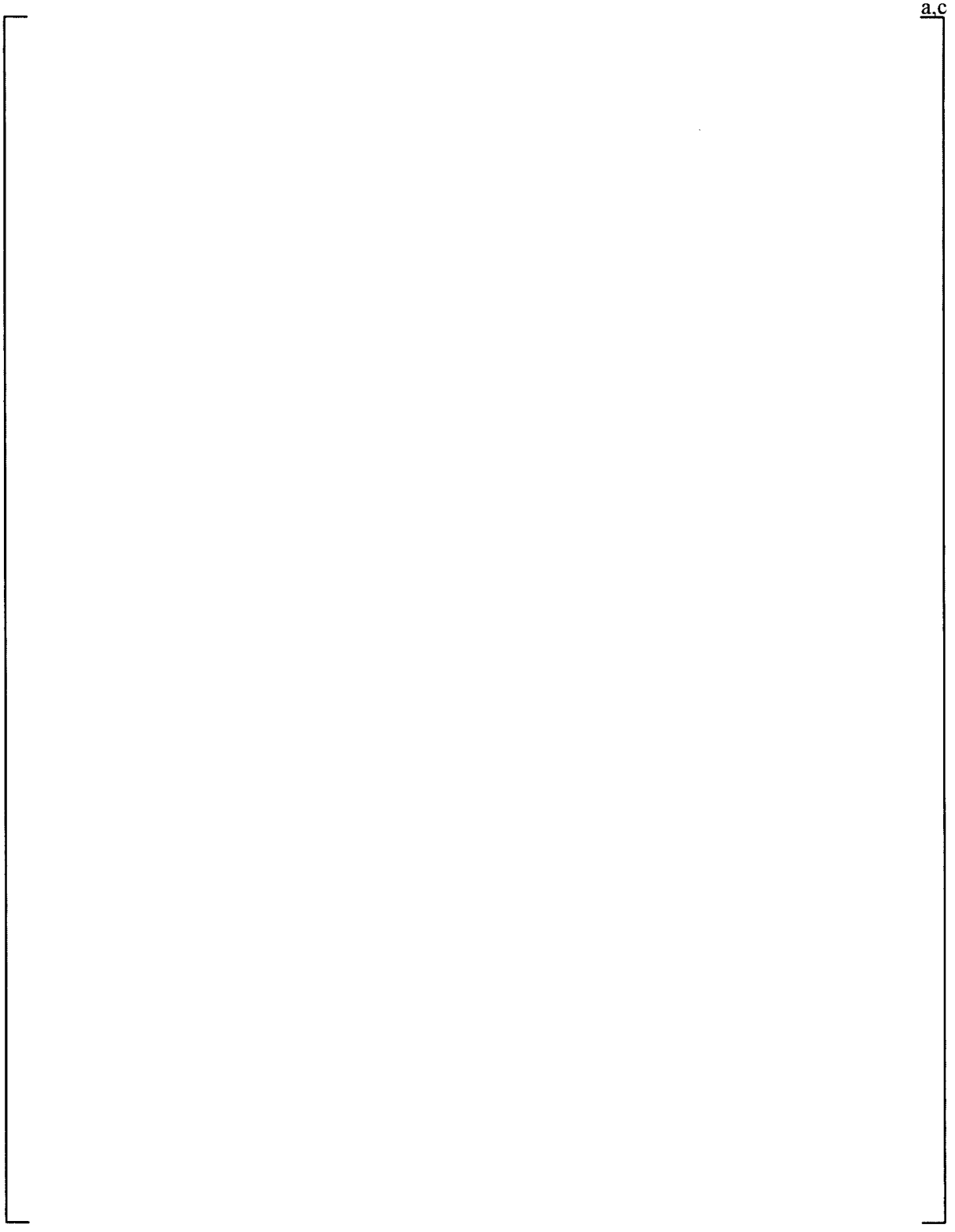

Figure 3-11 Peach Bottom Unit 2 Steam Dryer FEM: [ ]^{a,c}

a,c

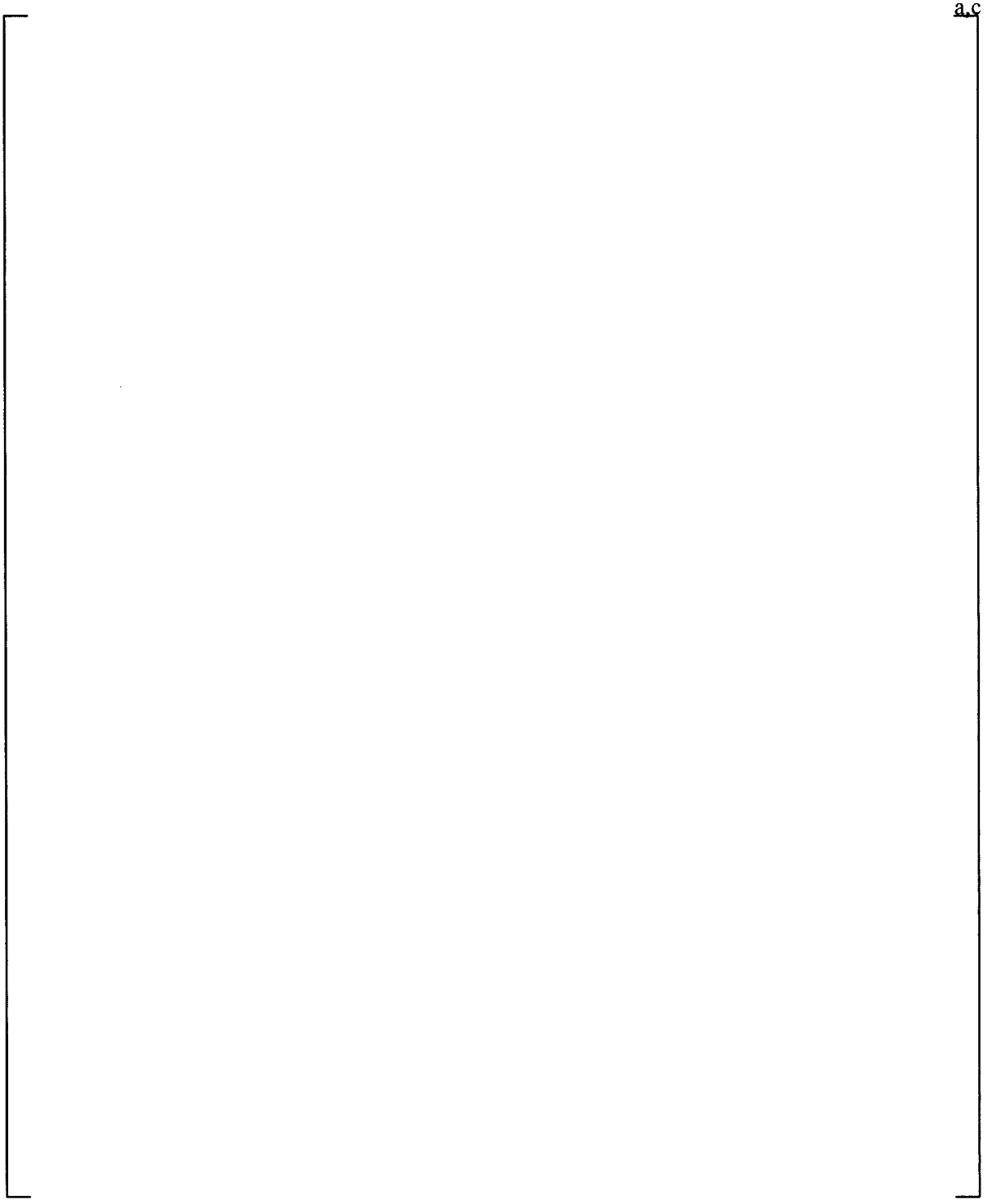

Figure 3-12 Peach Bottom Steam Dryer FEMs: [ ][a,c]

a,c

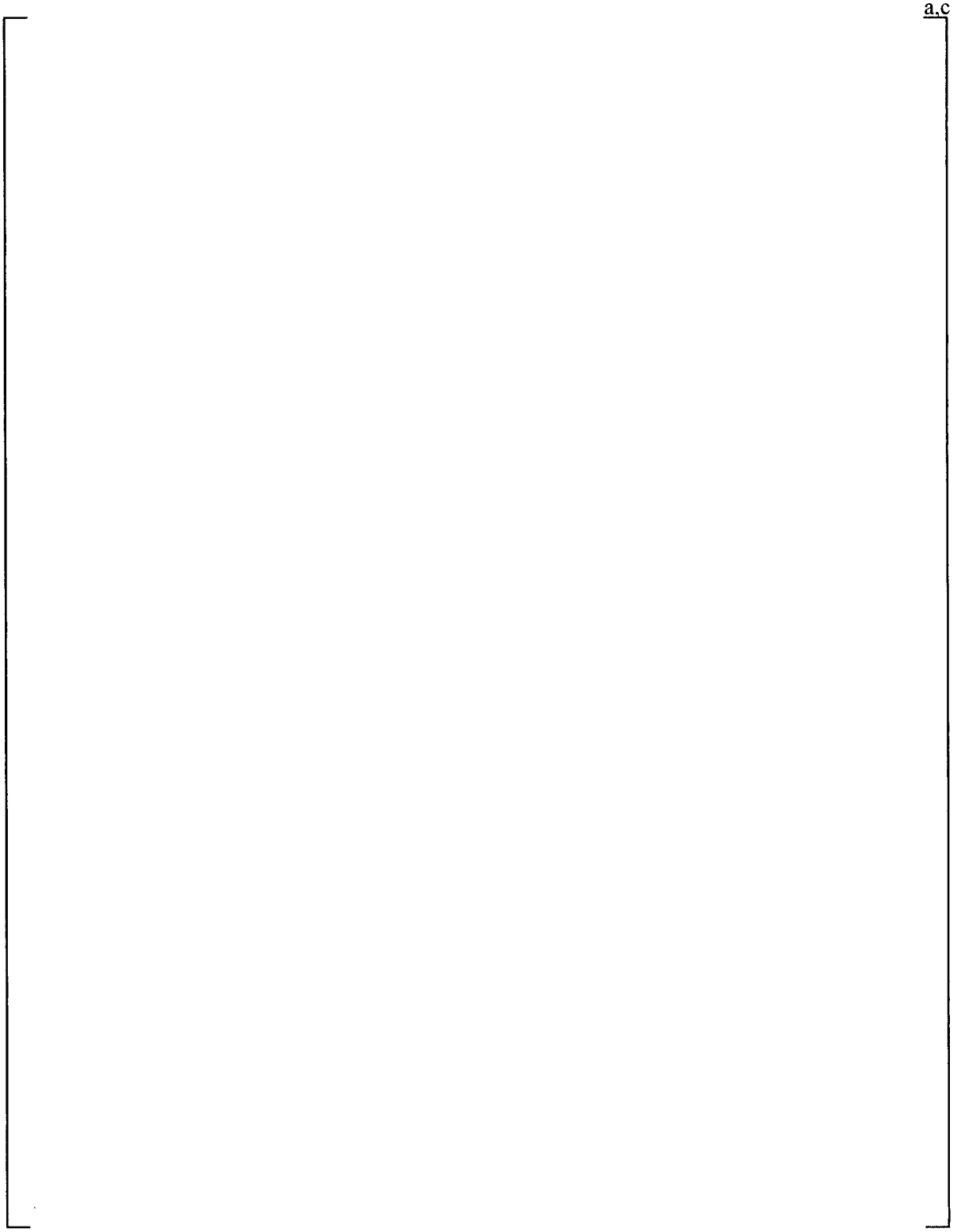

Figure 3-13 Peach Bottom Steam Dryer FEMs: [ ]^{a,c}

a,c

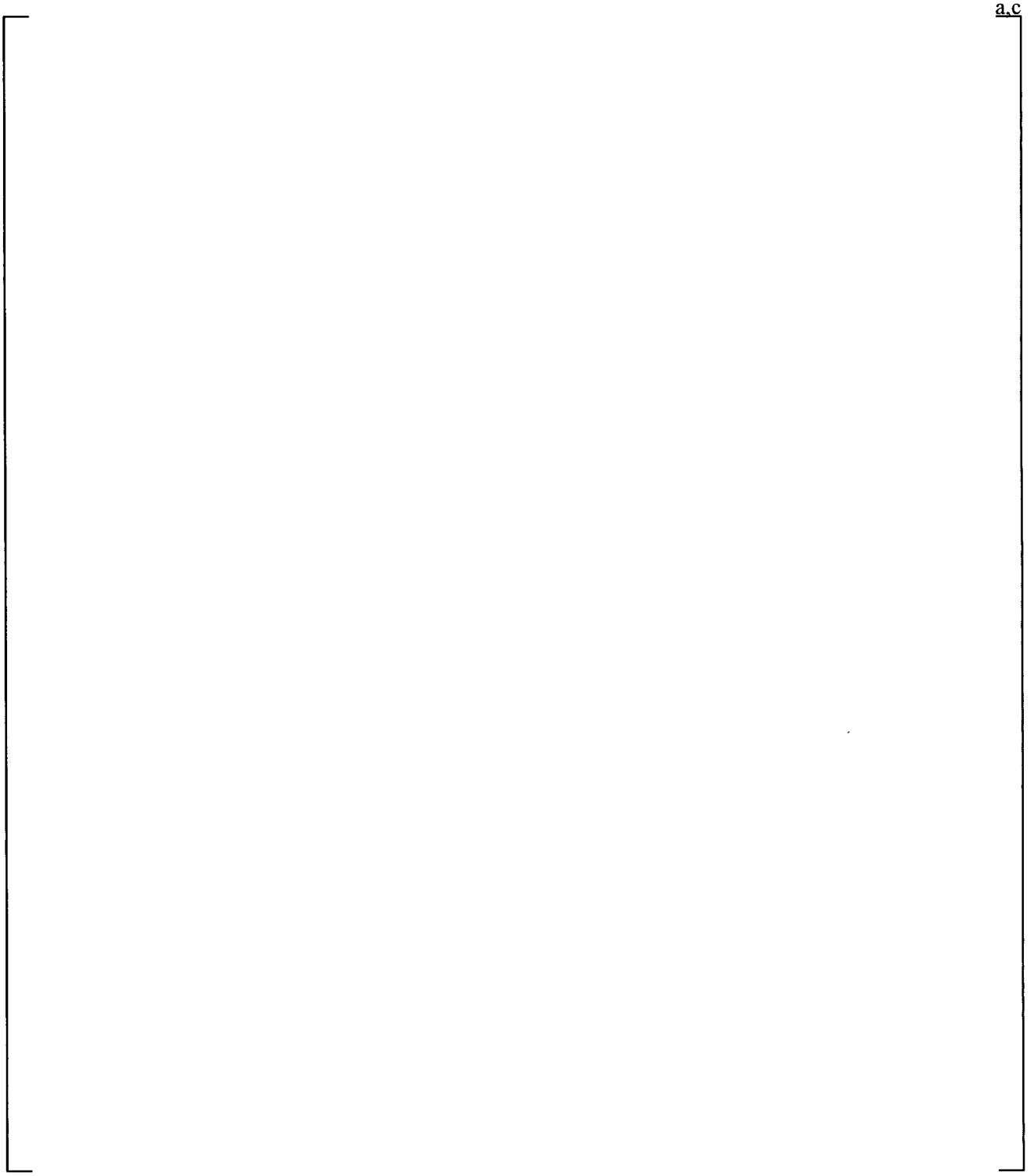

Figure 3-14 Peach Bottom Unit 3 FEM: [ ][a,c]

a,c

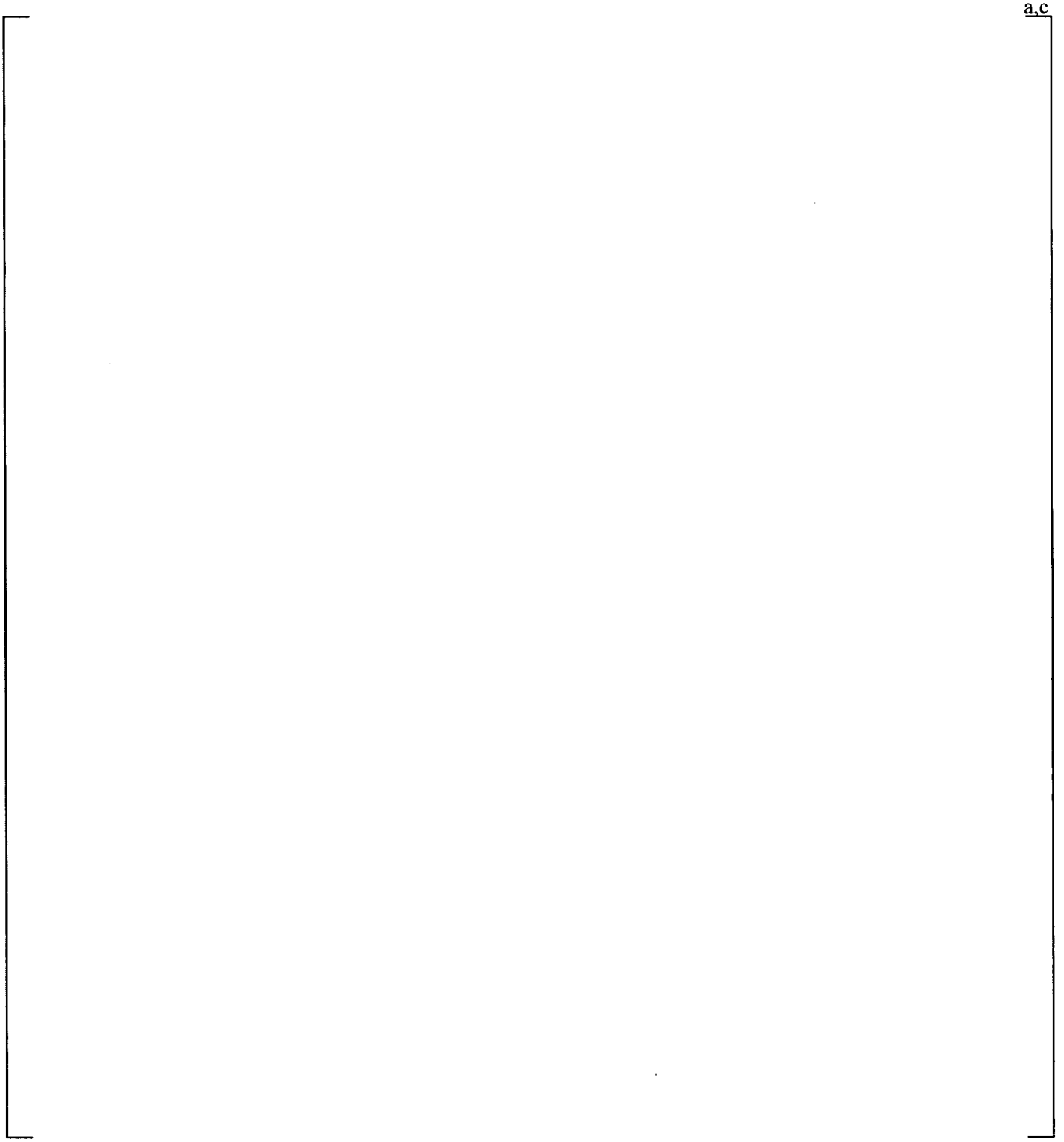

Figure 3-15 Peach Bottom Unit 2 with Mast: [ ]^{a,c}

a,c

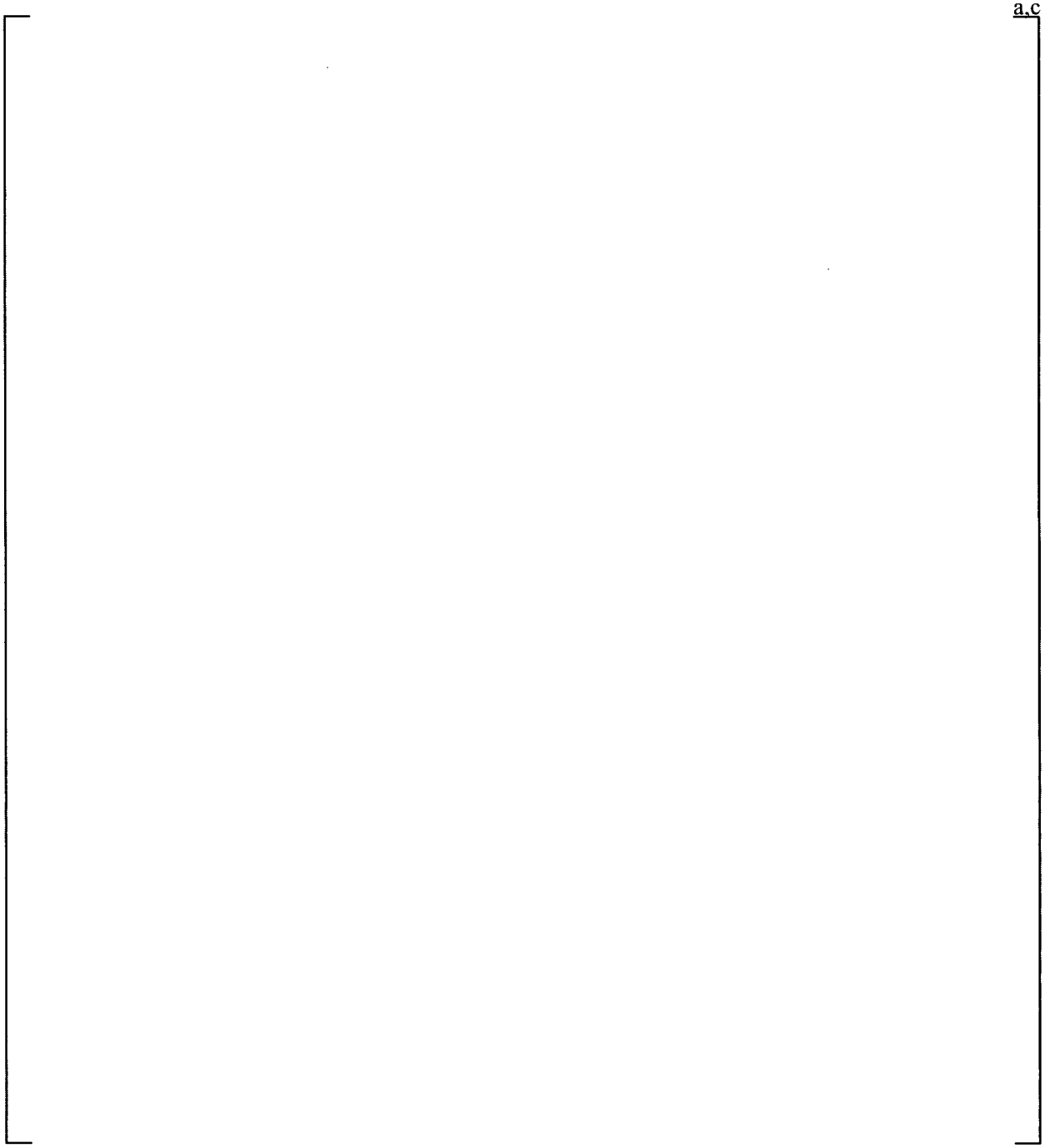

Figure 3-16 Peach Bottom Steam Dryer FEMs: Boundary Conditions [ ]^{a,c}

4 MATERIAL PROPERTIES

4.1 SUMMARY

A summary of the material properties used in the structural analysis is presented in Table 4-1. Material properties are taken from the ASME Code, Reference 1, for SS316L at the design temperature of 575°F.
[
]^{a,c} The perforated plates, located at the vane bank inlet, are modeled with equivalent plate properties to account for the reduced stiffness and mass of the plates. The density of the solid block representation of the vane banks is adjusted to achieve the correct overall mass of each vane bank. The stiffness of the mass block is [ ]^{a,c}.

4.2 STRUCTURAL DAMPING

Structural damping is defined as 1 percent of critical damping for all frequencies. This damping is consistent with guidance given on page 10 of NRC Regulatory Guide RG-1.20 (Reference 3). Using the harmonic analysis approach, a consistent damping level is used across the frequency domain.

Table 4-1 Summary of Material Properties a,c

Table 4-2 Summary of [ ]^{a,c} a,c

* Values adjusted to match detailed vane bank analysis.

5 MODAL ANALYSIS

As a precursor to performing the harmonic analysis, a modal analysis of the dryer was performed. The modal analysis was performed for modes between [ ]^{a,c}. Modal analysis of the dryer showed the expected natural frequencies and mode shapes of major dryer components such as hoods, skirt, and instrumentation mast and is consistent with previous modal analyses with other Westinghouse dryer analyses. Figures 5-1 to 5-6 show some selected dryer mode shapes at frequencies of interest. Inner hood mode shapes for frequencies between [ ]^{a,c} are shown in Figure 5-1. Selected mode shapes of the middle hoods are shown in Figure 5-2; included is a middle hood natural frequency at [ ]^{a,c}. Figures 5-3 and 5-4 show selected modes of the outer hood and skirt, respectively. Figure 5-5 shows modes of the vane bank top plate and Figure 5-6 shows selected PBAPS Unit 2 instrumentation mast modes. Both Figures 5-4 and 5-5 show modes at [ ]^{a,c}. The natural frequencies and mode shapes for the primary dryer panels were essentially identical for all three finite element models, with the exception of the lifting rod bracket and the instrumentation mast responses. Although the modal analysis is not directly used in the FIV dynamic analysis, the mode shapes and frequencies are used as one way to check the finite element model connectivity and material property assignments. This evaluation concluded that the finite element model is appropriate for use in the acoustic fatigue analysis.

a,c

Figure 5-1 Peach Bottom Unit 2 Modal Analysis: [ ]^{a,c}

a,c

Figure 5-2 Peach Bottom Unit 2 Modal Analysis: [ ]^{a,c}

a,c

Figure 5-3 Peach Bottom Unit 2 Modal Analysis: [ ]^{a,c}

a,c

Figure 5-4 Peach Bottom Unit 2 Modal Analysis: [ ]^{a,c}

a,c

Figure 5-5 Peach Bottom Unit 2 Modal Analysis: [ ][a,c]

a,c

Figure 5-6 Peach Bottom Unit 2 Modal Analysis: [ ]^{a,c}

6 LOAD APPLICATION

The frequency-dependent acoustic loads were developed using a three-dimensional (3-D) acoustic model representation of the dryer assembly (Figures 6-1 and 6-2). The acoustic pressure (P) loads on the replacement steam dryer structure were calculated by solving the 3-D wave diffusion equation in the frequency domain, i.e., the Helmholtz equation.

$$\nabla^2 P(\vec{r}) + k^2 P(\vec{r}) = 0$$

where:

k	=	ω/c is the wave number
ω	=	the angular frequency
r	=	a spatial variable
c	=	the speed of sound in the medium of interest

The resulting pressure loads are generated using a 1.5-inch uniform mesh grid. Loads are developed for both monopole and dipole load sources, and include both the real and imaginary portions of the load to maintain phasing information.

The acoustic load files have a frequency increment between solutions of [5]^{a,c} Hz. Using special-purpose computer codes, the frequency interval is reduced to limit the peak response error below 5 percent. This methodology results in variable frequency spacing across the frequency domain, with finer frequency spacing at the lower frequencies.

The acoustic load files generated in the acoustic analysis are input to a special-purpose computer program and the data reorganized into a 3-D table array format required for reading into ANSYS. The data from the acoustic analysis are limited to the grid positions of the acoustic model and only data adjacent to the replacement steam dryer surfaces are present in the files. In preparing the ANSYS load tables, interpolation of the data on the model surface and diffusion schemes off the surface are used to fully populate the load tables. The acoustic and finite element model coordinate systems are shown in Figures 6-3 and 6-4 (Reference 4).

To be consistent with the acoustic model, only surfaces of the structural FEM that are represented in the acoustic model are prepared to accept the pressure values from the table array files. The FEM is prepared by [

]^{a,c}.

[

]^{a,c} The loads for PBAPS Unit 2 and Unit 3 are different.

a,c

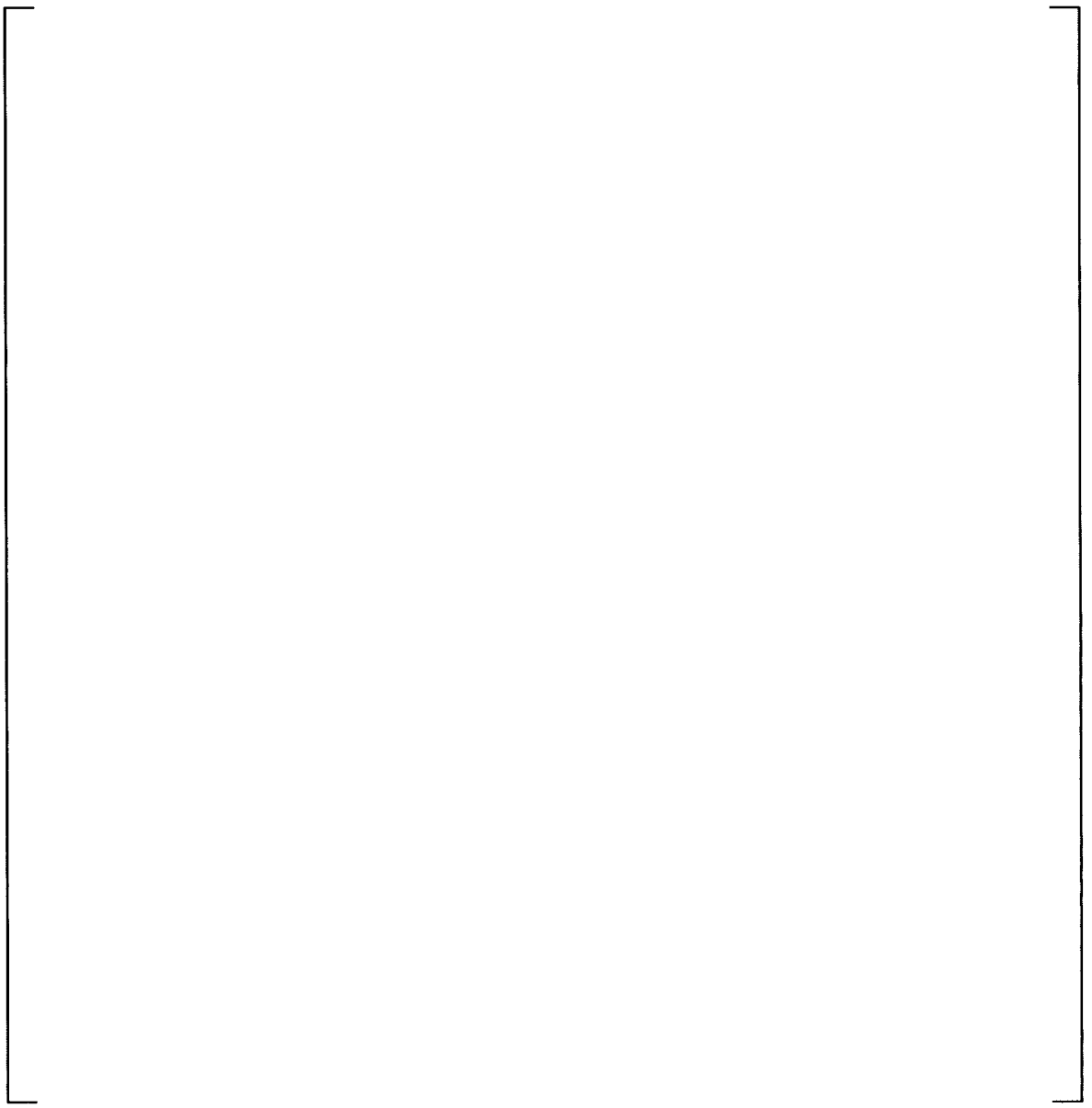

Figure 6-1 Peach Bottom RSD Acoustic Model – Cross Section

a,c

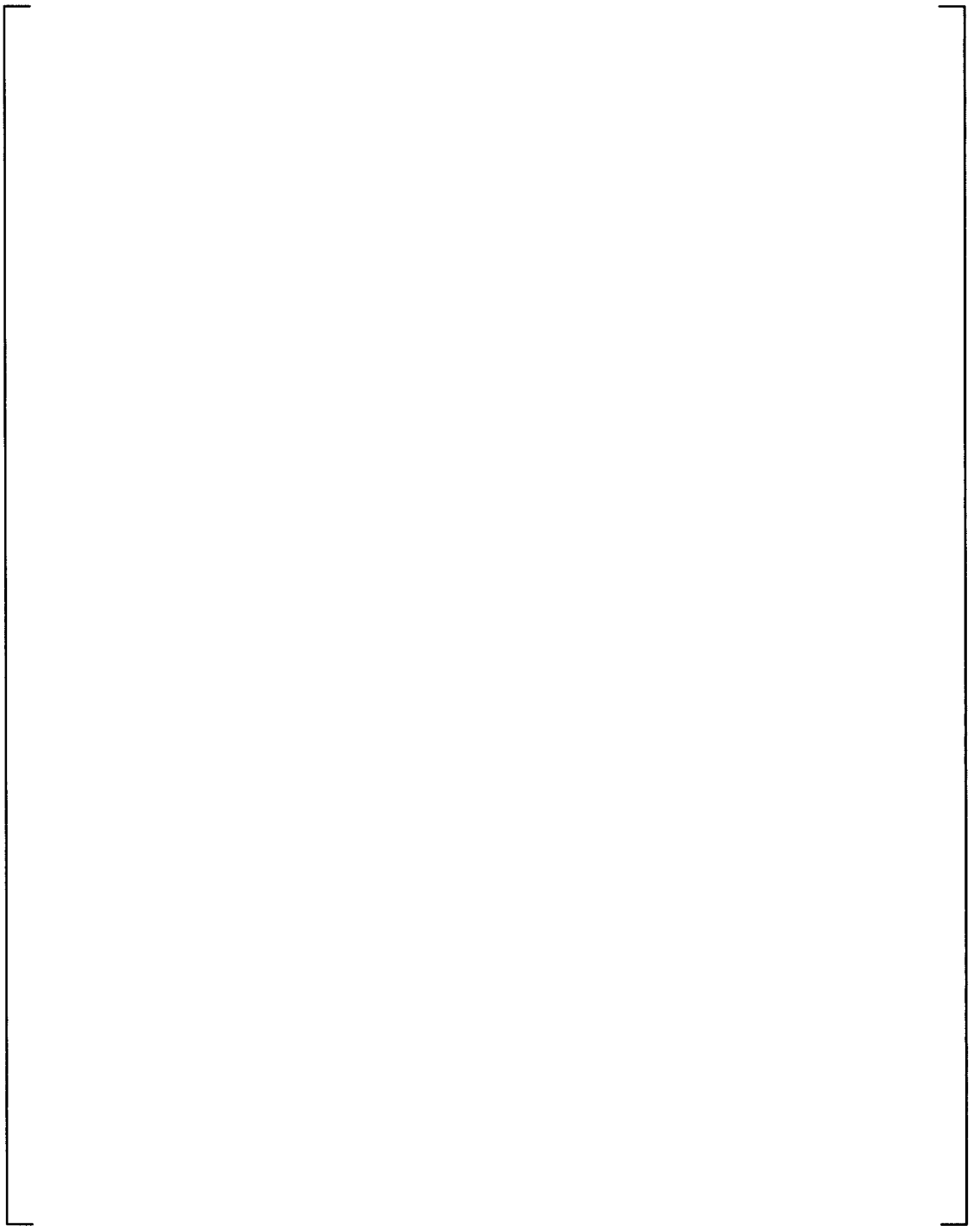

Figure 6-2 Peach Bottom RSD Acoustic Model – Three-Dimensional Views

a,c

Figure 6-3 ACM and FEM Global Coordinate System Layout, Top View

a,c

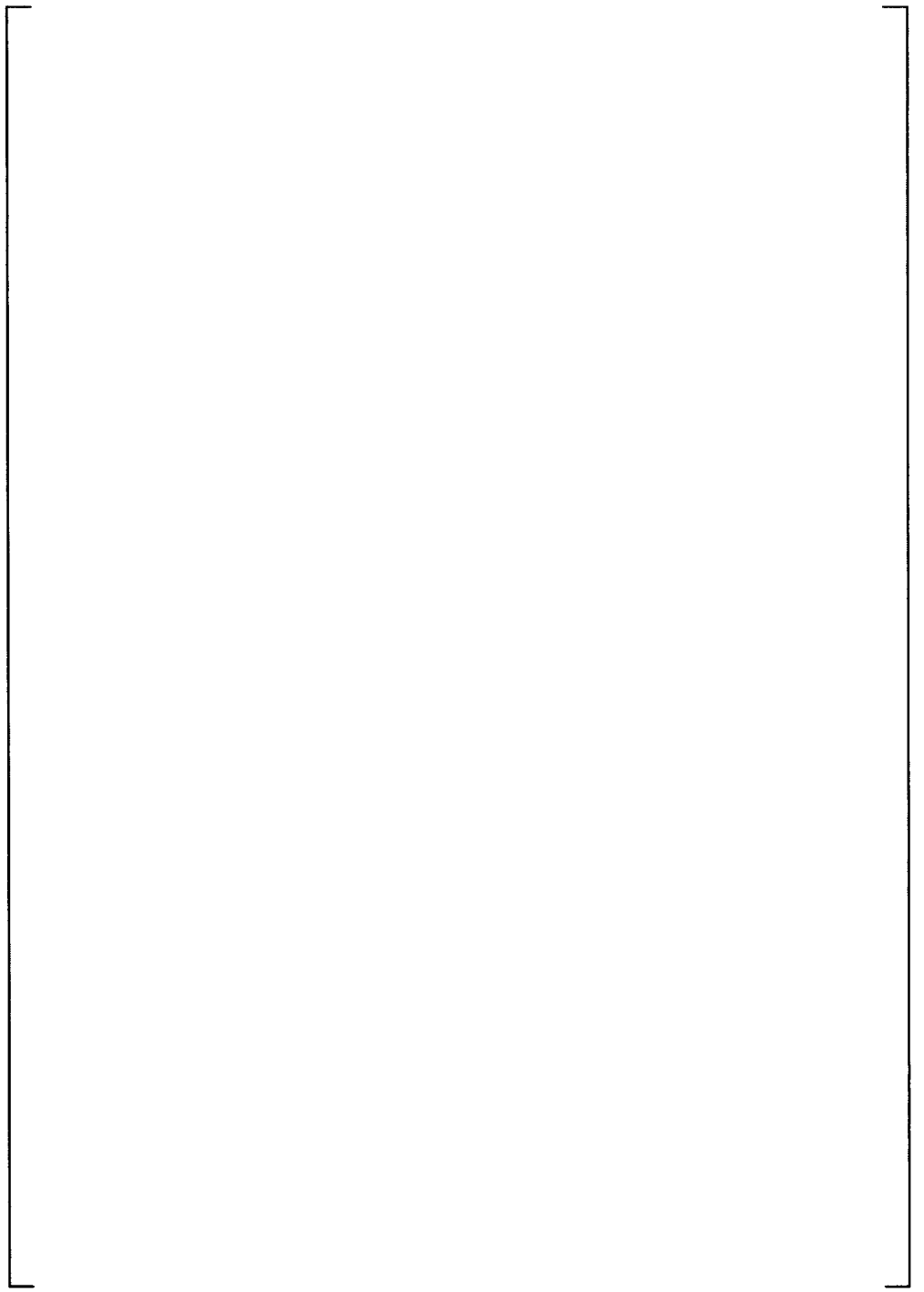

Figure 6-4 ACM and FEM Global Coordinate System Layout, Side View

7 STRUCTURAL ANALYSIS

7.1 HARMONIC ANALYSIS

7.1.1 Overview

The harmonic analysis begins with the [

]^{a,c} Separate solutions are obtained for [

]^{a,c}

7.1.2 Inverse Fourier Transform

[

]^{a,c}

[

]a,c

a,c

To calculate h_k, an IFT is performed.

7.1.3 Frequency Scaling (Shifting)

As a result of approximations of the structural interactions used in developing the FEM, small errors can occur in the prediction of the component natural frequencies. Varying degrees of mesh discretization can also introduce small errors in the FEM results. To account for these effects, frequency scaling is applied to the applied load history (Reference 2).

If frequency scaling is applied, [

]a,c

a,c

[

]a,c

a,c

7.2 POSTPROCESSING FOR PRIMARY STRESS EVALUATION

Once the time history has been calculated [ ]a,c, an evaluation is performed to calculate the maximum alternating stress intensity. The stress intensities for the [

]^{a,c}

For a two-dimensional stress field, the principal stresses are calculated as follows. (The X-Y plane is used as an example. The same algorithms are also applicable to other planes.)

$$\sigma_{1,2} = \frac{\sigma_x + \sigma_y}{2} \pm \sqrt{\left(\frac{\sigma_x - \sigma_y}{2}\right)^2 + \left(\sigma_{xy}{}^2\right)}$$

$$\sigma_3 = 0.0$$

$$\text{Stress Intensity} = \text{Maximum} \begin{vmatrix} |\sigma_1 - \sigma_2| \\ |\sigma_2 - \sigma_3| \\ |\sigma_3 - \sigma_1| \end{vmatrix}$$

For a general 3-D state of stress, the resulting principal stresses correspond to the roots of the following cubic equation as:

$$\sigma^3 - a_2\sigma^2 + a_1\sigma - a_0 = 0$$

where:

$$a_2 = \sigma_x + \sigma_y + \sigma_z$$
$$a_1 = \sigma_x\sigma_y + \sigma_y\sigma_z + \sigma_z\sigma_x - \sigma_{xy}{}^2 - \sigma_{yz}{}^2 - \sigma_{zx}{}^2$$
$$a_0 = \sigma_x\sigma_y\sigma_z + 2\sigma_{xy}\sigma_{yz}\sigma_{zx} - \sigma_x\sigma_{yz}{}^2 - \sigma_y\sigma_{zx}{}^2 - \sigma_z\sigma_{xy}{}^2$$

For such a general state of stress, there exist three stress invariants, I_1, I_2, and I_3. These stress invariants, expressed in terms of the resulting principal stresses, are expressed as follows:

$$I_1 = \sigma_1 + \sigma_2 + \sigma_3$$
$$I_2 = \sigma_1\sigma_2 + \sigma_2\sigma_3 + \sigma_3\sigma_1$$
$$I_3 = \sigma_1\sigma_2\sigma_3$$

The stress invariants are also identically equal to the constants, a_0, a_1, and a_2, such that:

$$I_1 = a_2$$
$$I_2 = a_1$$
$$I_3 = a_0$$

The general solution for a cubic equation is available in a number of references, such as Reference 5, and generally involves roots with both real and imaginary parts. In this case, it is known that all of the roots are real. In addition, the stress invariants provide a built-in self-check of the resulting principal stresses.

The membrane and bending stresses for beam elements are extracted at each end of the beam element. Bending stresses are stored about each of the local "Y" and "Z" axes. The membrane stress intensity is obtained directly from the results file. The maximum membrane plus bending stress intensity is calculated as follows:

$$\text{Stress Intensity} = \text{Maximum} \begin{vmatrix} \sigma_{xx} + \sigma_{YB} + \sigma_{ZB} \\ \sigma_{xx} + \sigma_{YB} - \sigma_{ZB} \\ \sigma_{xx} - \sigma_{YB} + \sigma_{ZB} \\ \sigma_{xx} - \sigma_{YB} - \sigma_{ZB} \end{vmatrix}$$

7.3 ALTERNATING STRESS

The calculation of the alternating stress intensity, following the ASME Code process, is performed as follows:

1. Calculate the range of stress for each component of stress for two time points.
2. Apply the stress concentration factors.

[

]^{a,c}

7.4 SUBMODELING

Due to the nature of the acoustic analysis and the large number of solutions that are required, it is not practical to use a fine mesh for the harmonic unit load analysis. Rather a mesh density is used that can accurately predict the dynamic characteristics of the structure, but may require some additional analysis for localized regions of high stress. Based on the results for the global model, [

]^{a,c}

The locations are based on results for the global models for Peach Bottom Unit 2 with and without instrumentation mast and Unit 3. [ ]^{a,c}

[

]a,c

7.5 FORCE EXTRACTION AND HANDBOOK CALCULATIONS AT WELDS

After all dryer components' minimum stress ratios (SRs) were compiled, the following locations were
[

]a,c

At selected locations with full penetration welds, forces were extracted from the harmonic solution results which were then used for hand calculating the stress intensity.

8 DYNAMIC ANALYSIS RESULTS SUMMARY

The results of the dynamic analysis of the replacement steam dryer are summarized for the global FEM welds and non-weld locations with stress ratios less than 4.0. The stress ratio reported for the dynamic analysis of the steam dryer is:

Stress Ratio = Allowable stress/Calculated stress

The allowable stress is the material fatigue endurance limit (13,600 psi) and the calculated stress is:

Calculated Stress = ANSYS stress x Elastic Modulus adjustment (Section 2.2.2) x SCF

The resulting minimum stress ratios for the dryer are summarized for components with stress ratios less than 4.0 in Tables 8-1, 8-2 and 8-3 for Peach Bottom Unit 2, Peach Bottom Unit 3, and Peach Bottom Unit 2 with the instrumentation mast, respectively. [

]^{a,c}

Stress contour plots from the global model for selected components are included in Figures 8-1 through 8-14 for Peach Bottom Unit 2, Figures 8-15 through 8-27 for Peach Bottom Unit 3, and Figures 8-28 and 8-29 for Peach Bottom Unit 2 with the instrumentation mast. The stresses in the contour plots in Figures 8-1 through 8-29 are the stresses taken directly from ANSYS before the elastic modulus adjustment and stress concentration factor have been applied. The calculated stresses in Tables 8-1 through 8-3 have all of these factors applied and are the final stresses used in calculating the stress ratios. Therefore, the stress values in the contour plot legends will not be the same as those reported in the results tables.

8.1 [ ]^{a,c}

[

]^{a,c}

8.2 [ ]^{a,c}

[

]^{a,c}

[

]a,c

8.3 [ ]a,c

[

]a,c

8.4 [ ]a,c

[

]a,c

Table 8-1 Peach Bottom Unit 2 Stress Results Summary

a,c

Table 8-2 Peach Bottom Unit 3 Stress Results Summary

a,c

Table 8-3 Peach Bottom Unit 2 with Instrumentation Mast Stress Results Summary

a,c

a,c

Figure 8-1 Peach Bottom Unit 2, [ ]^{a,c}

a,c

Figure 8-2 Peach Bottom Unit 2, [ ]^{a,c}

a,c

[

]

Figure 8-3 Peach Bottom Unit 2, [ ]^{a,c}

a,c

Figure 8-4 Peach Bottom Unit 2, [ ]^{a,c}

a,c

Figure 8-5 Peach Bottom Unit 2, [ ]^{a,c}

a,c

Figure 8-6 Peach Bottom Unit 2, [ ]^{a,c}

a,c

Figure 8-7 Peach Bottom Unit 2, [ ]^{a,c}

a,c

Figure 8-8 Peach Bottom Unit 2, [ ]^{a,c}

a,c

Figure 8-9 Peach Bottom Unit 2, [ ]^{a,c}

a,c

Figure 8-10 Peach Bottom Unit 2, [ ]^{a,c}

a,c

Figure 8-11 Peach Bottom Unit 2, [ ]^{a,c}

a,c

Figure 8-12 Peach Bottom Unit 2, [ ]^{a,c}

a,c

Figure 8-13 Peach Bottom Unit 2, [ ]^{a,c}

a,c

Figure 8-14 Peach Bottom Unit 2, [ ]^{a,c}

a,c

Figure 8-15 Peach Bottom Unit 3, [ ]^{a,c}

a,c

Figure 8-16 Peach Bottom Unit 3, [ ]^{a,c}

a,c

Figure 8-17 Peach Bottom Unit 3, [ ]^{a,c}

a,c

Figure 8-18 Peach Bottom Unit 3, [ ]^{a,c}

a,c

Figure 8-19 Peach Bottom Unit 3, [ ]^{a,c}

a,c

Figure 8-20 Peach Bottom Unit 3, [ ]^{a,c}

a,c

Figure 8-21 Peach Bottom Unit 3, [ ]^{a,c}

a,c

Figure 8-22 Peach Bottom Unit 3, [ ]^{a,c}

a,c

Figure 8-23 Peach Bottom Unit 3, [ ]

a,c

Figure 8-24 Peach Bottom Unit 3, [ ]^{a,c}

a,c

Figure 8-25 Peach Bottom Unit 3, [ ]^{a,c}

a,c

Figure 8-26 Peach Bottom Unit 3, [ ]^{a,c}

[a,c

]

Figure 8-27 Peach Bottom Unit 3, [ ]^{a,c}

a,c

Figure 8-28 Peach Bottom Unit 2 with Instrumentation Mast

a,c

Figure 8-29 Peach Bottom Unit 2 with Instrumentation Mast

[a,c]

Figure 8-30 Global Stress Results and Submodel Location – [ ]^{a,c}

a,c

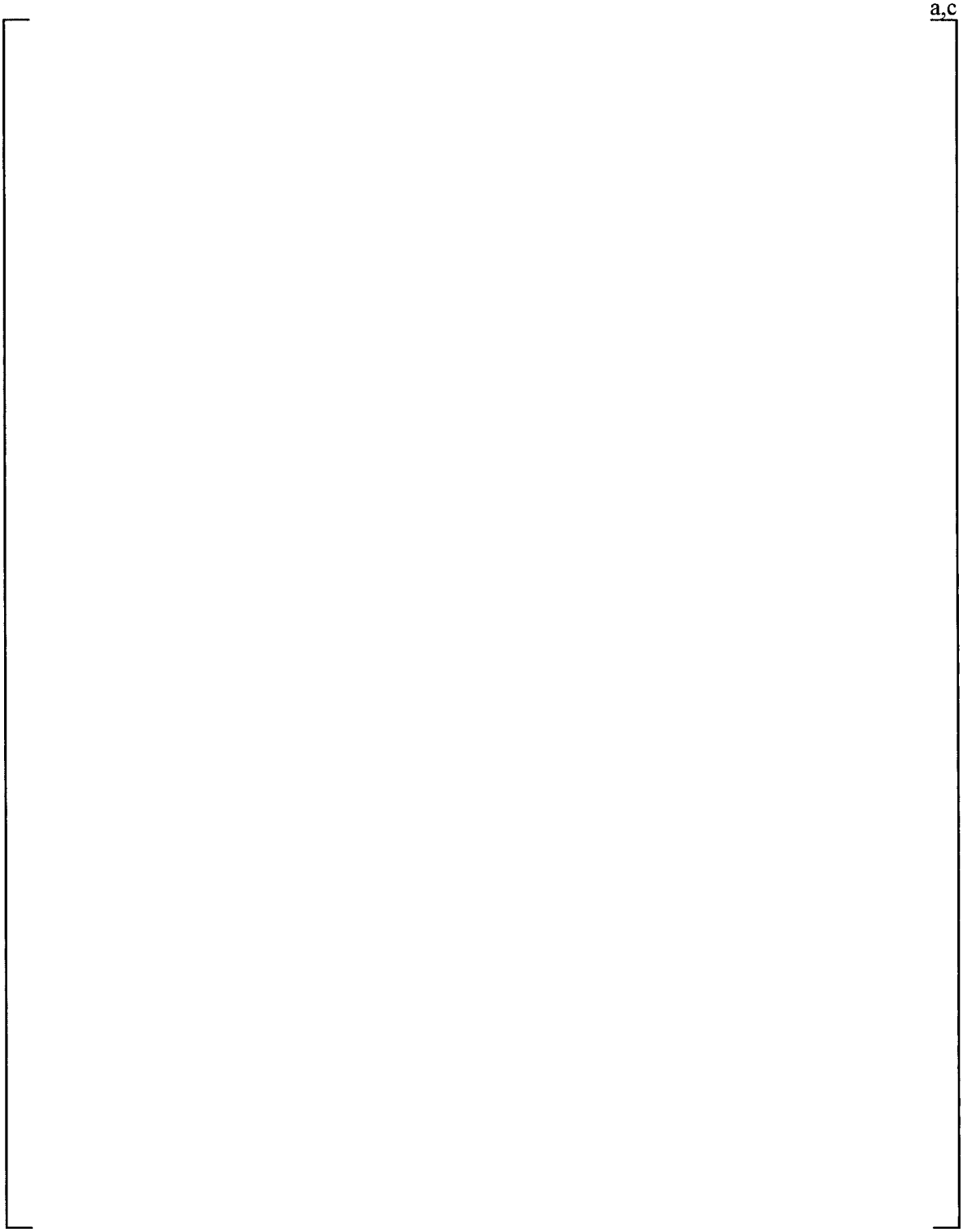

Figure 8-31 [ ]^{a,c} Mesh Diagram

[a,c

]

Figure 8-32 [ ]^{a,c} Stress Contour Plot

[a,c]

Figure 8-33 [ ]^{a,c} Weld Stress

a,c

Figure 8-34 [ ][a,c]

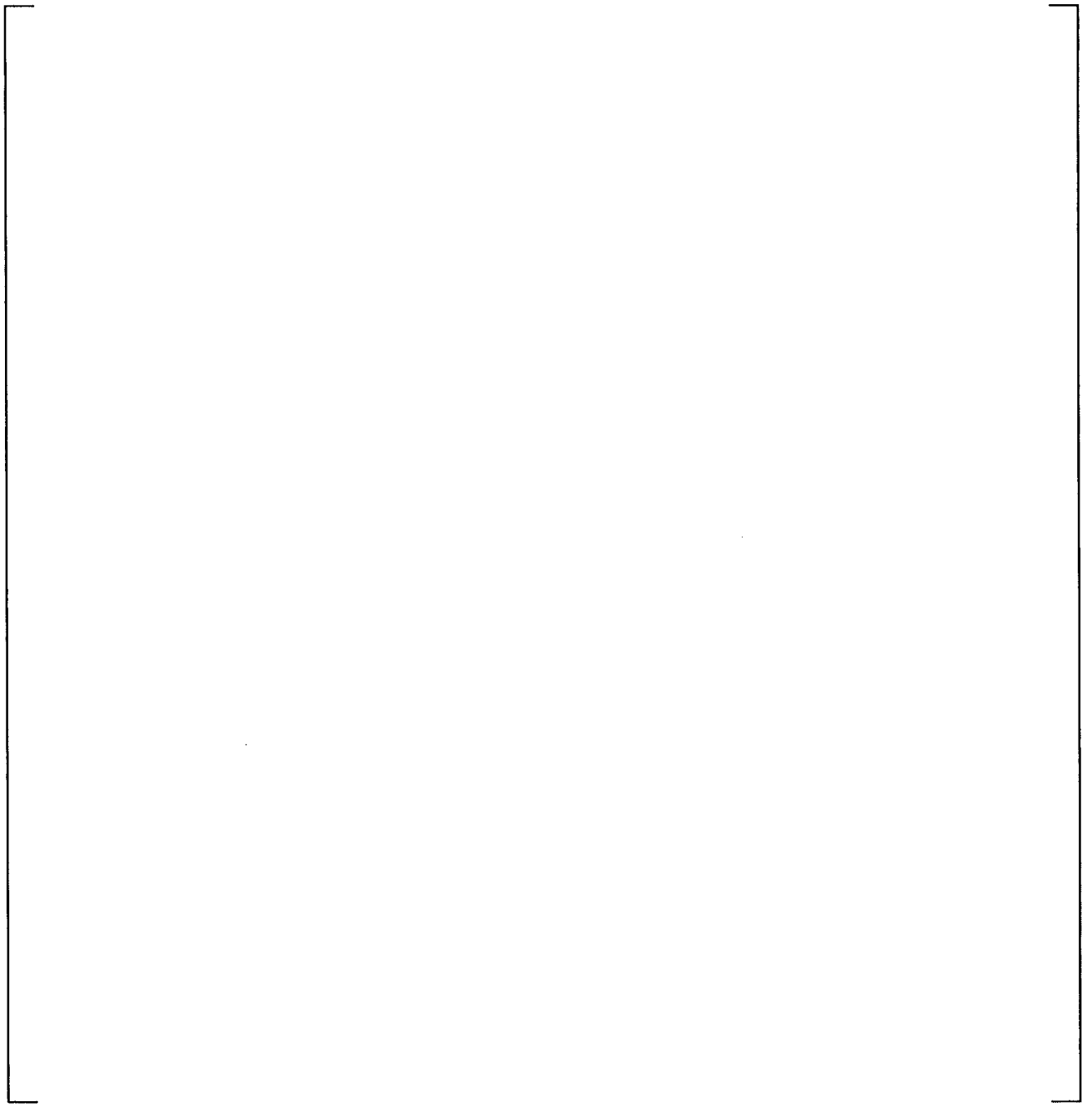

a,c

Figure 8-35 [ ]^{a,c} Mesh

[a,c]

Figure 8-36 Global Model Stress Results [ ]^{a,c}

a,c

[ ]

Figure 8-37 [ ][a,c]

a,c

Figure 8-38 Global Stress Results and Submodel Location

a,c

Figure 8-39 [ ]^{a,c} Stress Results

a,c

Figure 8-40 Global Model Stress Results for [ ]^{a,c}

a,c

Figure 8-41 Global Model Stress Results at [ ]^{a,c}

a,c

Figure 8-42 [ ]^{a,c} Stress Results [ ]^{a,c}

a,c

Figure 8-43 [ ]^{a,c} Results at [ ]^{a,c}

9 SUMMARY OF RESULTS AND CONCLUSIONS

A high-cycle fatigue evaluation of the PBAPS Units 2 and 3 RSDs has been performed using loads generated from Revision 4.1 of the acoustic circuit model. Three acoustic resonance peaks have been observed in plant data obtained from the main steam lines (MSLs). These frequency peaks occur at [

]^{a,c}. Acoustic loads and stresses for EPU*1.02 conditions have been evaluated for high-cycle fatigue. The results of this evaluation indicate that the replacement steam dryer at EPU*1.02 plant conditions will meet the ASME B&PV Code Section III, Subsection NG high-cycle criteria. In addition, the results of this evaluation indicate that the replacement steam dryer at EPU*1.02 plant conditions will meet the present U.S. NRC guidelines. These results account for all the end-to-end biases and uncertainties in the loads, finite element model, and finite element analysis. Uncertainties in the modal frequency predictions of the FEM are accounted for by including the stresses computed for loads that are shifted in the frequency domain by [ ]^{a,c}.

10 REFERENCES

1. ASME Boiler and Pressure Vessel Code, Section II and Section III, 2007 Edition including 2008 Addenda.

2. *Guidance for Demonstration of Steam Dryer Integrity for Power Uprate.* Electric Power Research Institute, Palo Alto, CA: May 2010. BWRVIP-182-A.

3. Regulatory Guide 1.20, Rev. 3, "Comprehensive Vibration Assessment Program for Reactor Internals During Preoperational and Initial Startup Testing," U.S. Nuclear Regulatory Commission, March 2007.

4. WCAP-17590-P, Rev. 0, "Peach Bottom Units 2 & 3 Replacement Steam Dryer Acoustic Load Definition," August 2012. (Westinghouse Proprietary)

5. W.H. Press, "Numerical Recipes – The Art of Scientific Computing," 2nd ed., Cambridge: Cambridge University Press, 1992.